ACS POLYMERS Au
AN OPEN ACCESS JOURNAL OF THE AMERICAN CHEMICAL SOCIETY

pubs.acs.org/polymerau

Review

Light-Mediated Polymerization Induced by Semiconducting Nanomaterials: State-of-the-Art and Future Perspectives

Yifan Zhu and Eilaf Egap*

Cite This: *ACS Polym. Au* 2021, 1, 76–99

Read Online

ACCESS | Metrics & More | Article Recommendations

ABSTRACT: Direct capture of solar energy for chemical transformation via photocatalysis proves to be a cost-effective and energy-saving approach to construct organic compounds. With the recent growth in photosynthesis, photopolymerization has been established as a robust strategy for the production of specialty polymers with complex structures, precise molecular weight, and narrow dispersity. A key challenge in photopolymerization is the scarcity of effective photomediators (photoinitiators, photocatalysts, etc.) that can provide polymerization with high yield and well-defined polymer products. Current efforts on developing photomediators have mainly focused on organic dyes and metal complexes. On the other hand, nanomaterials (NMs), particularly semiconducting nanomaterials (SNMs), are suitable candidates for photochemical reactions due to their unique optical and electrical properties, such as high absorption coefficients, large charge diffusion lengths, and broad absorption spectra. This review provides a comprehensive insight into SNMs' photomediated polymerizations and highlights the roles SNMs play in photopolymerizations, types of polymerizations, applications in producing advanced materials, and the future directions.

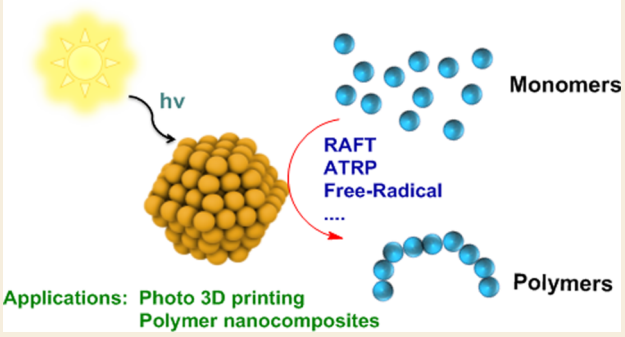

1. INTRODUCTION

Harvesting light as a trigger for polymerizations provides unprecedented advantages including abundant solar energy sources, low energy consumption, and mild reaction conditions and therefore represents advanced techniques for macromolecular synthesis.[1,2] The earliest examples of photopolymerization mainly focused on nonliving radical and cationic polymerizations,[3,4] while nonliving polymerizations usually suffer from low initiation efficiency and broad molecular weight (MW) distribution. In contrast, recent progress in controlled/living polymerization techniques, especially controlled radical polymerization (CRP), has revolutionized the synthesis of macromolecules by offering polymers with complex architectures, tunable molecular weights, and narrow MW distributions.[5−7] The integration of photomediated methodology with controlled polymerizations provides additional advantages such as high chain end fidelity and temporal/spatial control over polymerization.[2,8−13] The polymerization process could be simply controlled by switching the light "on" and "off". Indeed, the light-mediated process has been successfully incorporated into various polymerization systems including atom transfer radical polymerization (ATRP),[14−18] cationic polymerizations,[19−21] nitroxide-mediated radical polymerization (NMP),[22] ring-opening polymerization,[13,23] and reversible addition−fragmentation chain-transfer (RAFT) polymerization.[24−30]

One of the key components in photopolymerization systems is the photoresponsive species, which we named photomediators. Photomediators can be mainly divided into two categories according to their functions in the reaction, which are photoinitiators (PIs) and photocatalysts (PCs).[2] PIs are usually responsible for initiating polymerization with little control over the propagation and termination process and usually result in nonliving polymerizations. On the other hand, PCs could mediate the activating/deactivating process in the living polymerization via photocatalytic cycles and thus have emerged as a powerful tool to synthesize polymers with high precision of chemical composition and to manufacture complex polymeric materials.[8,31−34] Due to the recent explosion of interest in photoinduced polymerizations, a large number of photomediators, including organic small molecules[8,15,16,20,21,27,30,35−37] and metal complexes,[17,38−41] have been demonstrated to establish efficient photopolymerization systems and have revolutionized light-mediated

Received: May 27, 2021
Published: August 5, 2021

https://doi.org/10.1021/acspolymersau.1c00014
ACS Polym. Au 2021, 1, 76–99

polymerization by exploring oxygen tolerance,[42] lowering the catalyst loading,[43] expanding the scope of monomers,[44−46] and others.[47−49] Therefore, the development of easy-to-produce photomediators that could afford polymer products with complex architectures and targeted MW is of general interest.

In the past 30 years, the development of semiconducting nanomaterials (SNMs) has demonstrated numerous breakthroughs in many fields such as bioimaging,[50] light-emitting diodes,[51] and solar cells.[52] With a typical size ranging from 1 to 100 nm, the shape of SNMs can also vary from one dimension to three dimensions. Starting from inexpensive raw materials, SNMs can easily be synthesized and purified with different surface chemistry, sizes, crystal structures, and compositions, exhibiting tunable band gaps and energy levels.[53] Moreover, SNMs also have large extinction coefficients (>10^5 M^{-1} cm^{-1}),[53] broad absorption spectra,[54] and multiple molecular binding points.[55,56] These characteristics make SNMs a promising class of photomediators. Indeed, SNMs have been reported as robust PIs/PCs for CO_2 reduction,[57] water splitting,[58] and small-molecule transformation.[59,60] Although SNMs appear to be an excellent alternative to metal complexes and organic PCs, little attention has been paid to the SNM-catalyzed photopolymerization.[61] Furthermore, because nanotechnology and polymerization science are two different research areas, a broad scope of knowledge and experiment skills are required for conducting the study in SNM-induced photopolymerization, which also restricts its development.

Currently, although there are a number of excellent reviews on photopolymerization,[2,4,8,9,11,37,62−64] a few specific reviews focus on SNM-induced photopolymerization.[61,65,66] Therefore, the aim of this review is to highlight the state-of-the-art progress of using SNMs in regulating photopolymerizations, especially radical polymerizations, summarize its applications in controlled polymerization, and provide some future perspectives. We also included some polymerization examples of recently developed photoresponsive NMs such as noble metal nanoparticles (NPs). We elucidated the roles of SNMs in photopolymerization by focusing on mechanistic aspects, classified the types of SNMs and photopolymerization methodologies that have been reported in this field, and demonstrated their applications in the preparation of advanced polymeric materials.

2. ROLE OF SNMS IN THE REACTION

As we discussed in the Introduction, photomediators are divided into two categories including PIs and PCs in the past reviews of photopolymerization.[2] In this review, we further classify the function of SNMs in photoinduced polymerizations into the following three categories: PIs, photoactivators/photosensitizers, and PCs, based on the polymerization mechanisms.

2.1. SNMs as Photoinitiators

When the excited-state SNMs directly activate the monomer and initiate the polymerization process without the assistance of other co-initiation species, we can define the SNMs herein as PIs. Notably, the definition of photoinitiators in this review is slightly different from the previous report,[2] as we do not include the SNMs which could photoinitiate polymerization in the presence of co-initiators. We argue that the polymerization in the presence of co-initiators is actually initiated by radical species from the co-initiators instead of SNMs, and the role of SNMs in the polymerization system is actually photoactivating/sensitizing the co-initiators and thus should be considered as photoactivators, which will be thoroughly demonstrated in section 2.2. The currently proposed initiation mechanism using SNMs as PIs mainly involves three possible pathways upon photoexcitation (Scheme 1): (A) direct

Scheme 1. SNMs as Photoinitiators in Photopolymerizations: (a) Reduction of Monomer via Electron Transfer from Conduction Band, (b) Oxidation of Monomer via Hole Transfer from Valence Band, and (c) Radical Generation on the SNMs' Surface (CB Is the Conduction Band and VB Is the Valence Band)

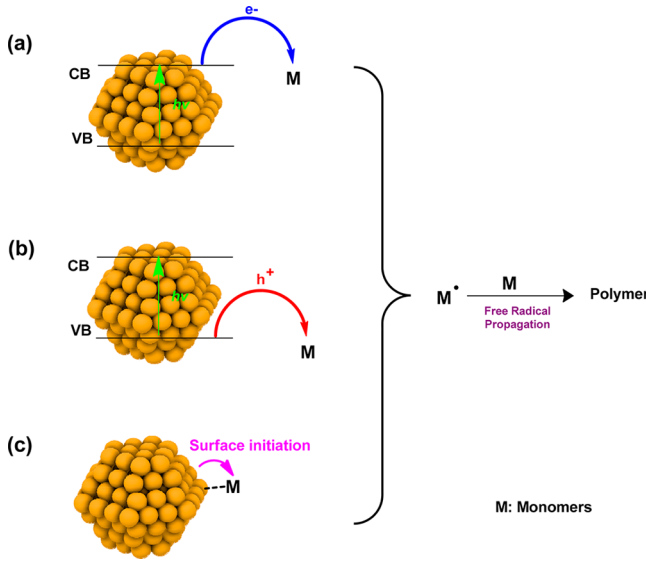

reduction of a monomer via electron transfer from SNMs' conduction band (CB);[67] (B) direct oxidation of a monomer via hole transfer from SNMs' valence band (VB);[68,69] and (C) radical generation on the SNMs' surface to initiate the monomers.[70] Mechanisms (A) and (B) require the SNMs with suitable band gap energy to ensure the charge transfer is thermodynamically favorable. For example, the reduction of methyl methacrylate requires a redox potential of <−2.1 V vs SCE, whereas oxidation could occur with a valence band of SNMs more positive than +2.0 V vs SCE.[70] Mechanism (C) occurs via a charge transfer from the anion-localized surface of SNMs to the monomer, which requires the coordination between SNMs' surface and monomers.[71] Generally, most polymerizations conducted by direct activation of the monomers using SNMs are relatively inefficient, with monomer conversion usually less than 20%.[67,68,70]

Apart from SNMs, noble metal NPs, such as gold (Au) and silver (Ag),[72,73] can also directly activate monomers via surface plasmon resonance (SPR)-induced hot electron transfer. Upon irradiation, a high concentration of energetic electrons whose energy levels are above Fermi level and strong electric fields are formed on the surface of the metal NPs.[74] These energetic electrons can then be transferred and activate the monomers close to the surface and induce photopolymerization.[75,76] Limitations of this method include the following: (1) the polymerization is restricted to the surface, thus hindering scale-up reactions, and (2) direct excitation of hot electrons usually requires large incident light intensities.[74]

https://doi.org/10.1021/acspolymersau.1c00014
ACS Polym. Au 2021, 1, 76−99

2.2. SNMs as Photoactivators

When the polymerization system consists of multiple initiating components (tertiary amines, RAFT agents, etc.) besides SNMs, photoexcited SNMs are used to transfer charges to those species, which could further initiate the polymerizations. We can thus define SNMs in this polymerization system as photoactivators or photosensitizers. Scheme 2a illustrates the general mechanism of SNM-photoinduced polymerization by sensitizing co-initiators. Based on their redox potentials, co-initiators can accept either excited electrons or holes from SNMs to provide radical sources for initiating monomers, followed by a free-radical chain-growth polymerization. Typical co-initiators include tertiary amines,[70,77] iodonium salts,[78−80] and alcohols,[79,81−86] which are molecules that can be easily oxidized or reduced to generate radical sources. On the other hand, redox mediators, such as RAFT agents[87] and the Cu(II) complex,[88] are usually compounds used for regulating controlled polymerizations under thermal or photoinitiation.[89] Particularly for photopolymerization, RAFT agents could be initiated via a photointerfier process, reacting with active radicals originating from photoinitiation or directly being reduced by PCs.[90] Similarly, the copper catalyst could be reduced to the low oxidation state by the excited photosensitizer,[91] which could further react with alkyl bromide initiators. For example, Scheme 2b presents a typical mechanism of photo-ATRP in the presence of SNMs and $CuBr_2$. Generally, the excited-state SNM could reduce Cu(II) to the active species Cu(I), which could react with alkyl halides and initiate the polymerization (Scheme 2b). In contrast to the uncontrolled propagation process induced by co-initiators, precise mediation of reversible activation/deactivation process could be achieved using redox mediators, operating polymerization in a controlled fashion and resulting in polymers with narrow molecular weight distribution (around 1.20).[88] However, since SNMs do not directly participate in the activation−deactivation cycle, residual catalysts may lead to the loss in temporal control.[92]

Scheme 2. SNMs Serve as Photoactivators in the Presence of (a) Co-initiators for Conventional Free Radical Photopolymerization and (b) Redox-Mediator-Controlled Photopolymerization

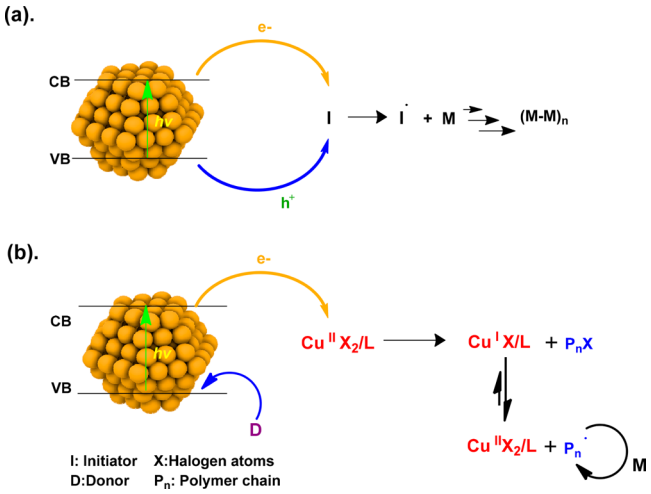

2.3. SNMs Serve as Photocatalysts

Photocatalysts are capable of donating or accepting electrons to/from other substrates under light irradiation, and they can also be relaxed to the ground state by accepting back charge transfer from the reaction systems in order to form a catalytic cycle.[8] The typical mechanism of photocatalyzed polymerization is shown in Scheme 3. Starting with photoexcitation, SNMs directly reduce the initiators or polymer chain ends via photoinduced electron transfer, forming active radicals. The radicals can either propagate with monomers or transfer electrons back to SNMs to complete the catalytic cycle. The charge transfer is restricted between SNMs and initiators/polymer chain ends, and therefore, SNMs can directly participate in mediating the reversible deactivation equilibrium. This newly established methodology[93] aims to conduct photocontrolled/living radical polymerizations, as the photocatalytic cycle induces reversible deactivation equilibrium,[1,17] providing well-defined polymeric structures and excellent temporal control over polymerization. Notably, sacrificial agents (electron/hole donors) could also be used to help with the regeneration of catalysts.[28]

Scheme 3. SNMs Serve as Photocatalysts in Photopolymerizations

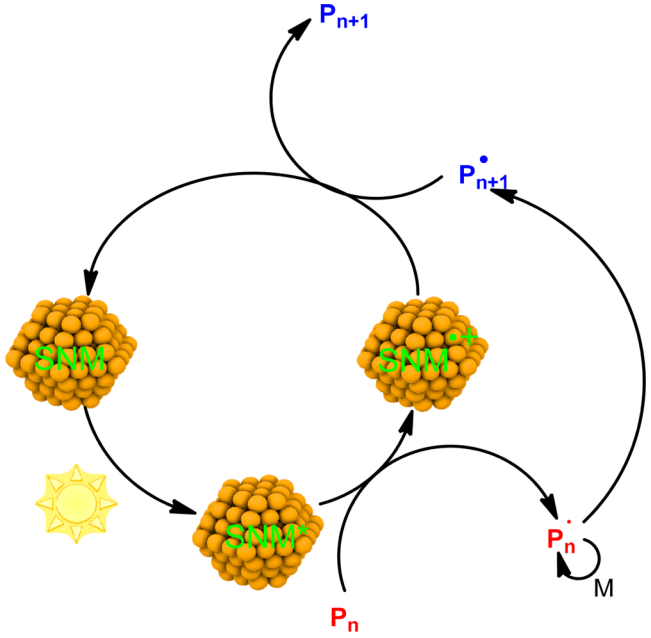

P_n: Polymer chains with living chain ends
M:Monomers

3. SNMS USED IN PHOTOPOLYMERIZATION

We highlighted in this section representative classes of SNMs which have been explored for photopolymerization. We also discuss the main characteristics of different materials including absorption wavelength, extinction coefficient, typical size, band gap energy, photoluminescence (PL) lifetime, and energy levels of the CB/VB. Some important examples are summarized in Table 1.

3.1. Metal Oxides

Metal oxide SNMs including titanium dioxide (TiO_2), zinc oxide (ZnO), iron oxide (Fe_2O_3), and tungsten oxide (WO_3) have shown excellent photocatalytic performance in water

https://doi.org/10.1021/acspolymersau.1c00014
ACS Polym. Au 2021, 1, 76−99

Table 1. Examples of Optical and Electronic Properties of SNMs

category	examples	absorption onset (nm)	band gap (eV)	emission (nm)	PL lifetime (ns)	CB (eV)	VB (eV)
metal oxide	ZnO[94]	380	3.2	*a*	*a*	−4.30	−7.50
	Bi_2O_3[94,95]	440	2.8	400−440[96]	0.94[97]	−4.60	−7.40
metal chalcogenide	CdSe (3.3 nm)[93]	565	2.3	575	16−22[98]	−3.21	−5.55
	CdS (3.7 nm)[99]	420	2.95	550	15−20[100]	−3.80	−6.80
perovskite nanocrystal	$CsPbX_3$[101] (X = Cl,Br, I)	420−665	1.99−2.97	425−680	1−29[102]	−3.26 to −3.45	−6.24 to −5.44
metal-free SNM	carbon QDs[103−105]	380−420	3.1−3.5	510−560[b]	2.81−48.7	∼2.0	∼−5.2

[a]Emission varies with different luminescence mechanisms; please see the reviews for further detail.[106,107] [b]Excitation wavelength of 458 nm.

splitting and carbon dioxide reduction due to their excellent photosensitivity and stability.[61] However, as metal oxides are usually wide-band-gap semiconductors,[61] the absorption of metal oxide SNMs is limited mainly in the UV region. For example, the band gaps of TiO_2 and ZnO are both 3.2 eV.[108,109] However, UV light does not represent a significant part of the solar spectrum and usually leads to undesired side reactions such as monomer self-initiation.[12] On the other hand, Bi_2O_3 has been demonstrated to be an efficient PC for controlled polymerization under visible light[95,110] due to the small band gap around 2.8 eV.[94] Moreover, Bi_2O_3 also offers additional advantages such as inexpensive raw materials, high stability, and low toxicity.[94]

3.2. Metal Chalcogenides

Metal chalcogenides are composed of at least one chalcogen anion and at least one electropositive metal element. Changing the chemical components of metal elements renders the band gap energies spanning from the near-infrared (PbS, PbSe, etc.) to the ultraviolet (ZnS and ZnSe, etc.) regions. Particularly, metal chalcogenide quantum dots (QDs), solution-dispersible nanocrystals, represent an emerging class of PCs for photoinduced organic synthesis.[99,111−115] The size of metal chalcogenide QDs could be controlled within 1−10 nm with a narrow distribution, providing large surface area to volume ratios for chemical transformation to happen.[116] High extinction coefficients (around 10^6 M^{-1} cm^{-1})[117] of the materials facilitate the reactions happening at extremely low catalyst loadings (usually less than 10^{-3} mol %).[111] Moreover, due to the quantum confinements, the reductive potential of metal chalcogenide QDs can be easily tuned in the range of 2 eV via changing the size of QDs,[118] enabling efficient photoinduced electron transfer to organic compounds.[119,120] For instance, the reduction potential of CdSe QDs can be tuned to −1.59 V vs SCE[111] with a diameter of 3.3 nm, which is sufficient to reduce the commonly employed ATRP initiators such as alkyl bromide which has an oxidation potential around 0.8 V vs SCE[15]).

3.3. Hybrid Semiconductor−Metal Nanoparticles

Hybrid semiconductor−metal NPs (HSMNPs) usually combine two or more disparate materials into a single semiconducting nanosystem, conjugated with at least a metal island (Au, Ag, etc.) growing on a semiconductor NP.[121] The synthetic control of HSMNPs offers a high degree of control over the shapes, sizes, compositions, and morphologies of HSMNPs,[121,122] which allows the easy control of the semiconductor band gap, adjustment of the relative energetics level to optimize the charge separation, and alternation of the dispersibility of HSMNPs in diverse matrices.[123] Another advantage of HSMNPs as a photomediator is that the presence of the metal domain highly enhances efficient spatial charge separation, thus reducing charge recombination and significantly enhancing the photocatalytic ability of HSMNPs.[124] For example, cadmium sulfide hybrid nanorods with gold tips (CdS-Au) (5.1 ± 0.6 nm diameter of the nanorods and a total length of 30 ± 3 nm) have a first excitonic peak at 460 nm, with an extremely large molar extinction coefficient at 385 nm (10^7 M^{-1} cm^{-1}).[85] The metal domain was aimed to enhance the photoinduced charge separation by accepting electrons from nanorods and therefore preventing the charge recombination.[124] The enhanced electron−hole charge separation in HSMNPs facilitates effective photoinduced charge transfer, which leads to a faster polymerization rate and higher monomer conversion than that in bare NP counterparts.[124]

3.4. Perovskite Nanocrystals

Perovskite semiconducting materials have revolutionized the fabrication of advanced materials such as photovoltaics[125] and light-emitting diodes[126] due to their excellent optoelectronic properties including narrow emission band (full width at half-maximum <20 nm),[127] high PL quantum yields (up to 90%),[128,129] large extinction coefficients (around 10^6 M^{-1} cm^{-1}),[130] and long charge diffusion lengths (>175 μm).[131] These outstanding optoelectronic properties also make perovskite SNMs good candidates for PCs.[132,133] For example, the CB of lead halide (Cl, Br, I) nanocrystals (NCs) ranges from −1.24 to −1.54 V vs SCE and VB ranges from 0.71 to 1.47 V vs SCE,[101] making the charge transfer between NCs and most organic molecules thermodynamically favorable. Moreoever, the PL lifetime of $CsPbBr_3$ NCs ranges from 10 to 100 ns in various solvents,[102] which are sufficient for photoinduced charge transfer.[134] Currently, examples of perovskite photoinduced polymerization are very rare,[54,135−137] which might be caused by their instability toward water and air.[138−140]

3.5. Metal-Free SNMs

Developing metal-free catalysts for chemical transformations has attracted numerous attention in the past few years because of their low toxicity and cost efficiency.[10,37,141−143] Metal-free SNMs are mainly carbon-based materials with excellent photostability, low toxicity, and sustainable raw materials.[103] Metal-free SNMs such as carbon QDs,[103,144] nanostructured conducting polymers,[145] polymer nanofibers,[146] and micro-sized carbon nitride particles[147] have been developed for both controlled and free-radical polymerizations. Metal-free SNMs also process fascinating optical and electrical properties. For example, carbon dots (2−10 nm) exhibit an emission centered at 510 nm with a quantum yield of 8.82% upon irradiation at 458 nm.[103] Relatively strong absorption is usually observed in the UV region due to the n−π^* (C═O) transition in the core and on the surface of carbon QDs.[148] The fluorescence lifetime of carbon dots usually ranges from 1 to 10 ns,[103] which is sufficient for an efficient charge transfer to happen.[149]

https://doi.org/10.1021/acspolymersau.1c00014
ACS Polym. Au 2021, 1, 76−99

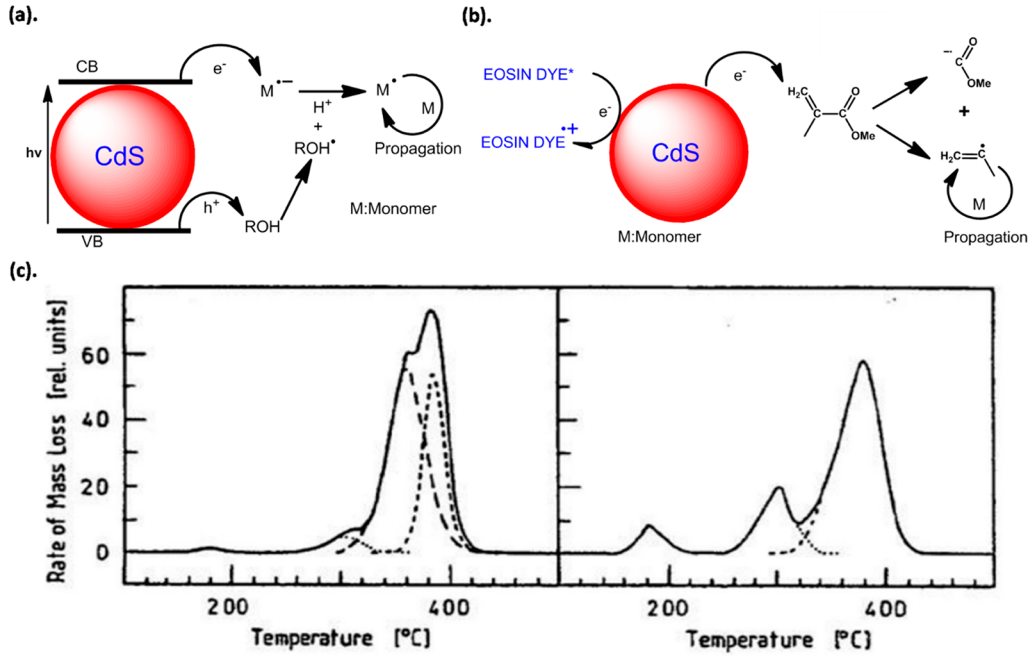

Figure 1. (a) Proposed mechanism of CdS NP photoinitiated polymerization via directly electron transfer from NPs to monomers. (b) Proposed mechanism of NP photoinitiated polymerization assisted by dyes under visible light. (c) DTG curves of PMMA prepared using CdS photoinitiated polymerization (left) and AIBN (right). Adapted with permission from ref 156. Copyright 1997 Springer Nature.

Furthermore, doping with heteroatoms such as phosphorus and sulfur could promote the photogeneration of electrons,[104] which is beneficial to the photocatalytic performance of carbon dots.

4. TYPE OF POLYMERIZATIONS PHOTOINDUCED BY SNMS

4.1. Nonliving/Conventional Free-Radical Polymerization

In this section, we introduce the free-radical polymerizations photoinduced by SNMs based on their charge transfer process and mechanisms.

4.1.1. Free-Radical Polymerization Directly Initiated by Photoinduced Charge Transfer from SNMs to Monomers. The earliest example of semiconducting material initiated free-radical polymerization can be traced back to the 1960s. Oster and Markham separately reported a photopolymerization initiated by ZnO under UV (λ = 365 nm) irradiation.[150,151] Methyl methacrylate (MMA) was successfully polymerized in the presence of oxygen. Authors proposed that light could produce an excited-state oxygen and form a radical anion on the surface of ZnO, which could initiate the monomer and propagate with a free-radical chain mechanism. The anion-initiated mechanism was further confirmed by electron paramagnetic resonance (EPR) studies. This hypothesis was also supported by the fact that polymerization could proceed with electrophilic monomers rather than with styrene.[151] In 1985, Kamat reported an n-type GaAs electrode photopolymerization of 1-vinylpyrene under visible light.[152] Due to the small band gap of GaAs electrodes (~1.4 eV), polymerization could be operated under visible light. The authors claimed that a hole could migrate from excited GaAs electrodes to monomer 1-vinylpyrene, forming an oxidized 1-vinylpyrene which could subsequently initiate the radical polymerization at the electrode surface.

Two of the disadvantages of the aforementioned bulk semiconductor materials are their small surface area and strong light scattering, which hinder the light absorption and consequentially limit the polymerization efficiency. Therefore, quantum-sized SNMs, which have a surface area to volume ratio higher than that of the bulk materials, were developed for photopolymerization to overcome these limitations. In 1992, Hoffmann and co-workers reported a radical polymerization of vinylic monomers photoinitiated by quantum-sized NPs including TiO_2, ZnO, and CdS in alkyl alcohol solvents upon the UV irradiation.[68,153] Significantly enhanced monomer conversion was observed for quantum-sized NPs (19%)[153] compared to that in their bulk counterparts (9%).[150] An anionic initiation mechanism followed by a free-radical propagation step was proposed (Figure 1a). The authors suggested that monomers could be reduced by photoexcited electrons at the CB on the surface of NPs, forming a radical anion which further initiated polymerization and propagated the monomers. This hypothesis was further confirmed by the fact that negligible polymerization was observed in the presence of oxygen or acetonitrile, which are known to interfere with radical anions. It is worthwhile to mention that the direct electron transfer from ZnO to monomers is not feasible because the CB of ZnO (−0.44 V vs SCE) is less negative than the reduction potential of monomers (−2.1 V vs SCE). The authors proposed that methyl methacrylates could be reduced by the electrons stored at the surface traps, and the surface traps possessed a very negative redox potential (<−2.24 V vs SCE). Further kinetics study by Mills on polymerization photoinitiated by annealed ZnO NPs also pointed out that reactions could preferentially take place at the NP surface.[154]

By introducing organic dyes as photosensitizers for SNMs, the chemisorbed or physisorbed dyes on the SNMs' surface could prolong the electron−hole separation[155] and thus significantly enhance electron transfer efficiency to the monomers. For example, eosin was reported to photosensitize

https://doi.org/10.1021/acspolymersau.1c00014
ACS Polym. Au 2021, 1, 76−99

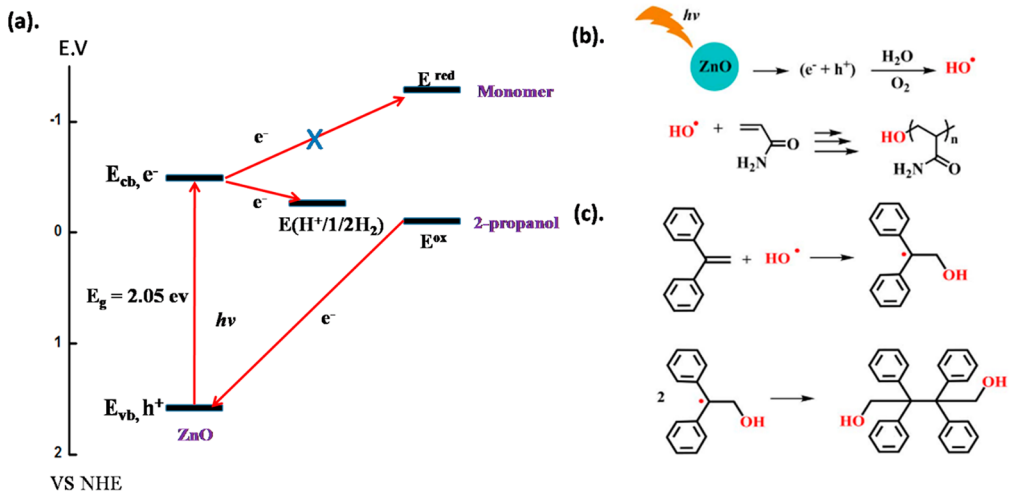

Figure 2. (a) Energy diagram and proposed charge transfer processes of the Fe_2O_3 photoinduced polymerization of BMA in the presence of 2-propanol. Adapted with permission from ref 83. Copyright 2001 Springer Nature. (b) Photopolymerization using ZnO NPs in aqueous phase. (c) Capturing $OH^•$ in a nonpolymerizable model reaction. Panels (b) and (c) are adapted with permission from ref 79. Copyright 2014 John Wiley and Sons.

CdS NPs under visible light.[155] Photoexcited electrons could be transferred from the eosin dye to the CB of semiconductors and subsequently relocate to the monomer for initiation polymerization (Figure 1b). A higher polymer yield was observed in the presence of eosin and CdS NPs (22%) compared to that in the CdS NPs (2%) alone, which was attributed to more free radicals generated by the dye-sensitized system.

Apart from anionic initiation induced by the electron transfer from excited-state SNMs to monomers, Popovic demonstrated a different initiation mechanism involving hole transfer from the VB to monomers.[156] Instead of reacting with the carbon double bonds on monomer molecules, the photoexcited CdS could oxidize MMA on the β-position through the hole transfer, abstracting a hydrogen atom and forming a stable acrylic radical which acted as an initiator and propagated monomers in a free-radical manner. This mechanism was supported by differential thermogravimetry (DTG) results (Figure 1c), where an additional peak and stronger thermal stability were observed in the poly(methyl methacrylate) (PMMA) samples obtained from CdS photoinitiated polymerization (Figure 1c, left) compared to sample thermal initiated by 2,2′-azobisisobutyronitrile (AIBN) (Figure 1c, right). The additional peak was attributed to the polymer with unsaturated chain ends, suggesting that polymerization might be initiated by acrylic radicals. A similar VB−hole initiation mechanism was reported by Ni and co-workers,[157] where polymerization of methyl methacrylate photoinitiated by nanosized TiO_2 semiconductors was established. Furthermore, because polymerization was conducted in the presence of oxygen, the authors also claimed that hydroxyl radical ($OH^•$) generated from the reaction between oxygen and electron−hole pairs could act as an initiation species.

4.1.2. Free-Radical Polymerizations Photoinduced by SNMs in the Presence of Co-initiators. One of the challenges for directly reducing monomers is that the reduction potential of acrylate-type monomers is very negative (around −2.1 V vs SCE),[70,153] which requires strongly reductive excited states of the SNMs and makes the reduction of monomers thermodynamically unfavorable. Therefore, co-initiators are introduced into polymerization systems to promote the generation of radical species and consequently enhance the initiator efficiency. Furthermore, co-initiators frequently act as electron donors/acceptors, which could suppress the charge recombination and improve the charge separation.

Alcohols are usually considered as the hole scavengers because of their small and negative redox potential (around −0.24 V vs NHE[83]). Indeed, many examples have employed alcohols as co-initiators to generate $OH^•$ for initiating chain propagation.[79,81−86] Kuchmii showcased a photopolymerization of butyl methacrylate (BMA) facilitated by hydrated ferric oxide (Fe_2O_3) NPs in the presence of 2-propanol.[83] Upon either UV or visible light irradiation, 2-propanol could donate an electron to the VB of excited Fe_2O_3 NPs (1.6 V vs NHE), generating active isopropoxy radicals capable of initiating a chain polymerization of BMA (Figure 2a). The fate of the excited electron was not probed in the study, but the authors suggested that it might be accepted by the proton formed during the oxidation of isopropyl alcohol. Moreover, $OH^•$ could also be yielded from photolysis of semiconductor NPs in water. In 2014, Yagci and co-workers reported a UV-light-induced polymerization of acrylamides initiated by both ZnO and iron-doped ZnO NPs in the aqueous environment.[79] A photoinduced electron−hole pair from NP-reduced water and molecular oxygen resulted in active $OH^•$ and thus initiated polymerization (Figure 2b). This mechanism is further evidenced by capturing $OH^•$ using an excess of 1,1-diphenylethylene in a nonpolymerizable model reaction (Figure 2c).

Although $OH^•$ could serve as an efficient co-initiator, performing polymerization in the typical $OH^•$ sources such as alcohols or water limits the scope of monomers polymerized via the methodology. Tertiary amines (TEAs), on the other hand, are the well-known sacrificial additives in photoinduced organic transformation.[38,93,158] TEA could form a radical cation by donating the lone pair electron on the N atom to the photogenerated hole, prevent back electron transfer from the CB to the VB, and meanwhile render the polymerization process in the organic medium. In 2012, Yagci reported a

https://doi.org/10.1021/acspolymersau.1c00014
ACS Polym. Au 2021, 1, 76−99

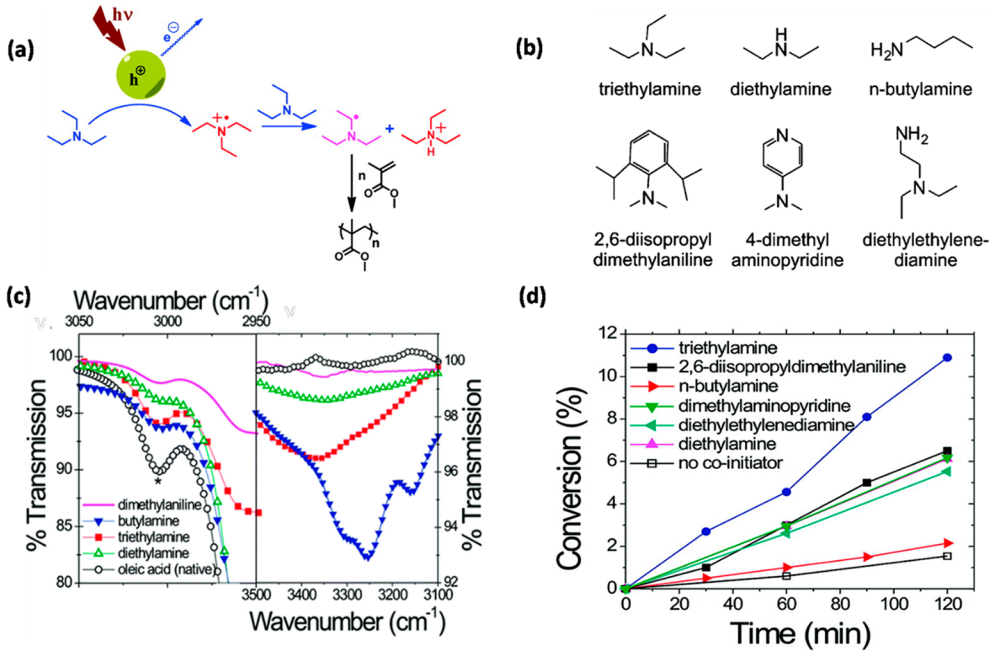

Figure 3. (a) Proposed initiation mechanism using mpg-C_3N_4 in the presence of amines. Adapted from ref 77. Copyright 2012 American Chemical Society. (b) Chemical structures of the co-initiators employed CdS QD-photoinduced neat polymerization. (c) FTIR transmission spectra of ligand-exchanged QD films. (d) Conversion of monomer versus time in the presence of different amines. Panels (b–d) are adapted from ref 70. Copyright 2008 American Chemical Society.

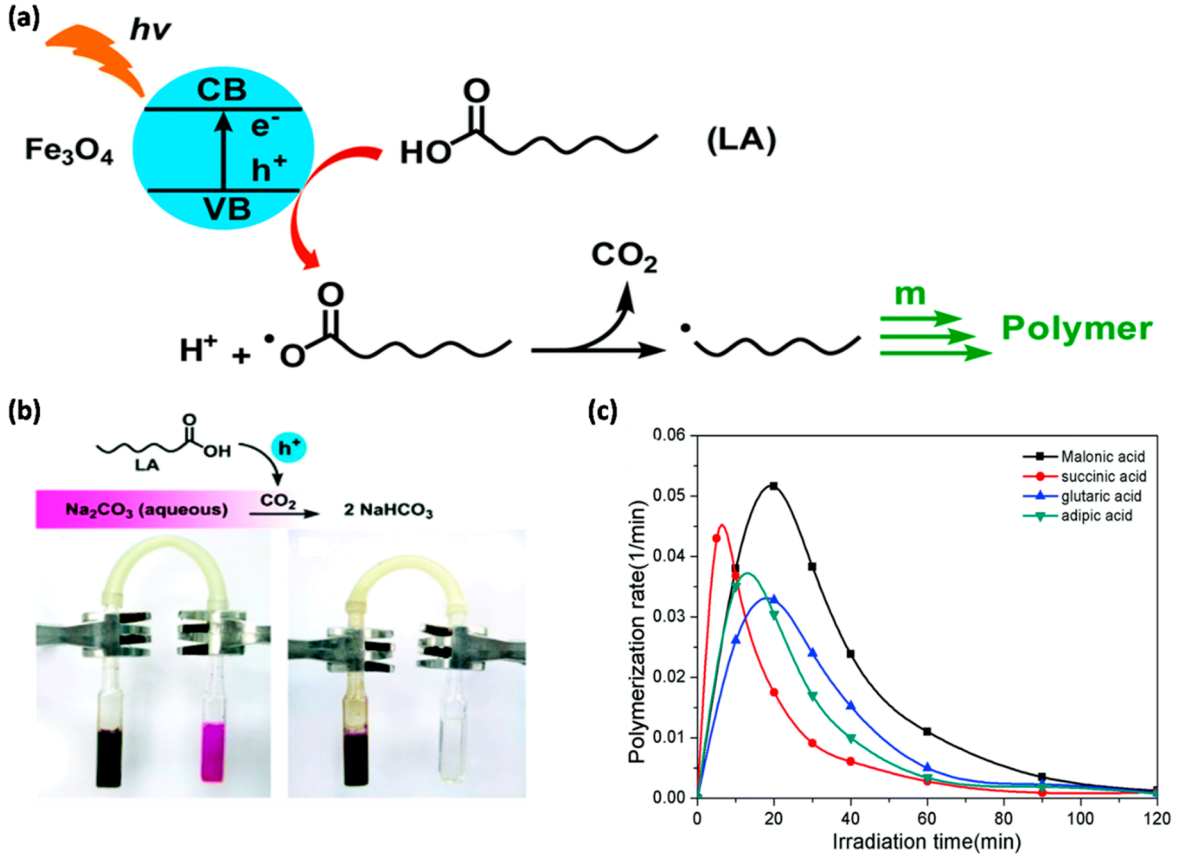

Figure 4. (a) Proposed mechanism for Fe_3O_4 nanoparticles photoinitiated polymerization of vinyl monomers with the LA surface agent. (b) Decarboxylation of LA using sodium carbonate with phenolphthalein in model reactions. Panels (a) and (b) are adapted with permission from ref 160. Copyright 2015 Royal Society of Chemistry. (c) Photopolymerization rate in the presence of different diacids. Adapted with permission from ref 164. Copyright 2017 Springer Nature.

https://doi.org/10.1021/acspolymersau.1c00014
ACS Polym. Au 2021, 1, 76–99

polymerization of MMA photoinitiated by mesoporous g-C_3N_4 (mpg-C_3N_4) in conjunction with tertiary amines.[77] Silica NPs are used as templates for C_3N_4, providing large surface areas as well as accessible surface sites for the photocatalysis process. The metal-free colloidal structure of mpg-C_3N_4 not only overcame the toxicity problem of metal oxide catalysts but also could be recovered and reused without losing catalytic performance. Amine was proposed to be oxidized by the photoexcited hole, form a radical cation, and subsequently abstract hydrogen from another amine to yield the initiating radical (Figure 3a). Another report by Stucky employed various amines (Figure 3b) in CdS semiconductor QDs to induce neat polymerization.[70] Amines with different structure parameters including the number and size of substituents and functional groups were examined. Fourier transform infrared spectroscopy (FTIR) transmission of different amine-treated QDs displayed that the native oleic acid ligands on CdS QDs could be replaced by amines (Figure 3c), where primary amines coordinate to semiconductor surfaces while secondary and tertiary amines possibly only remain weakly bound to the surface because of the low affinity and steric effect. Combining with the photoinitiation efficiency assisted by different amines (Figure 3d), the authors hypothesized that the removal of surface ligands increased the accessibility of the QDs' surface, consequently promoting photocatalytic activity of CdS QDs.[99,116] The highest initiation efficiency exhibited by the triethylamine system probably came from the faster electron-donating nature of triethylamine, and a more open QDs' surface resulted from the complete displacement of original ligands on the surface.

Surface ligands play an important role to confer solubility and prevent agglomeration for NPs.[159] Surface ligands such as lauric acid (LA) were found to interact with the photogenerated holes on magnetic iron oxide NPs upon visible light radiation (Figure 4a),[160] followed by decarboxylation and formation of initiating radicals. Decarboxylation of LA was further confirmed by carbon dioxide evolution in a model reaction without the monomer (Figure 4b). Schmitt and co-workers developed a photoinitiated bulk polymerization of multifunctional resins and acrylic esters using nanoscaled ZnO that are surface-functionalized with carboxylic acids.[161−163] The same decarboxylation reaction of carboxylic acids induced by the photoexcited electron−hole pair was proposed and confirmed by EPR and gas chromatography−mass spectrometry measurements. Successful radical photopolymerizations could be operated even under weak simulated illumination (365 nm light intensity ≈0.5 mW cm^{-2}).[163] Very recently, Ni's group demonstrated a free-radical polymerization of vinyl acetate photoinitiated by a binary mixture of TiO_2 NPs and carboxylic diacid.[164] Polymerization in aqueous conditions approached over 90% monomer conversion, which is much higher than that of bulk polymerization. The authors ascribed the superior performance to the high decarboxylation efficiency in water. Moreover, the polymerization rate was much more rapid using diacids with an even number of carbon atoms than odd number of carbon atoms (Figure 4c), as the former one is prone to coordinate with the NPs' surface in a bidentate pattern and thus accelerate the decarboxylation process. Such a decarboxylation−initiation process was also developed for utilizing butyric acid and TiO_2 NP as the co-initiator and photosensitizer, respectively.[165]

Apart from aforementioned SNMs' photoinitiated polymerization assisted by hole scavengers, electron acceptors such as onium salts (iodonium, sulfonium, etc.) could also function as the co-initiators to trigger polymerizations.[78−80] For example, iodonium salt could accept photoexcited electrons and separate into iodobenzenes and phenyl radicals, which subsequently initiate the chain propagation (Figure 5a).

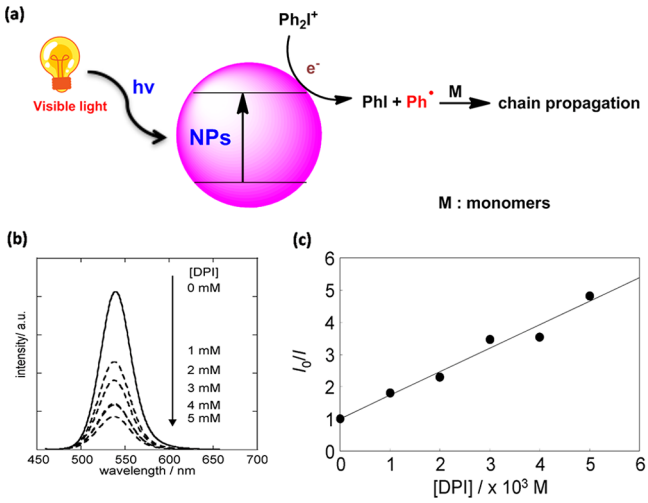

Figure 5. (a) Proposed photoinitiation mechanism in the presence of NPs and iodonium salts. (b) PL spectral change of CdTe NCs with the addition of onium salts. (c) Stern−Volmer plot of CdTe NCs emission quenching with onium salts. Adapted from ref 80. Copyright 2007 American Chemical Society.

Kawai and co-workers reported a photosensitized polymerization of ionic liquid-based monomers in the presence of CdTe NCs and an onium salt, diphenyliodonium hexafluorophosphate (DPI).[80] The photoluminescence quenching of CdTe NCs by DPI gave almost a linear Stern−Volmer relationship (Figure 5b,c), revealing a photoinduced electron transfer (PET) process from the excited NCs to co-initiators. Polymerization photosensitized by CdTe was so rapid that full conversion could be achieved within 1 min, which benefited from the large molar extinction coefficient and the long excitation lifetime of CdTe NCs. Notably, the polymerization was preferable to be conducted under visible light in order to avoid direct excitation of onium salts. Apart from SNMs, Au NPs were also developed as the photoinitiator for radical polymerizations of acrylic monomers in the presence of [4-[(octyloxy)phenyl]phenyl]iodonium hexafluoroantimonate as the co-initiator.[78] Thiol-stabilized Au NPs acted as electron donors upon excitation at the plasmon resonance band (λ > 450 nm), transferring electrons to iodonium salts which then decomposed into free radicals. After the plasmonic resonance electron was donated, the electron-poor Au core could accept another electron from stabilizing the ligand via intramolecular electron transfer.

4.1.3. Free-Radical Polymerizations Using SNMs via Surface-Induced Photoinitiation. Besides the redox process mentioned above, surface-coordination-induced charge transfer is also a facile route to initiate polymerization.[116] The strong Lewis acid metal atoms/cations at the surface are prone to coordinate with the double bond of monomers and donate electrons from the anion localized state. For instance, Tan's group reported recently a perovskite NC-initiated photopolymerization of vinyl monomers under white light illumination via a surface initiation mechanism.[136] The authors postulated that the olefin of the monomer could coordinate

https://doi.org/10.1021/acspolymersau.1c00014
ACS Polym. Au 2021, 1, 76−99

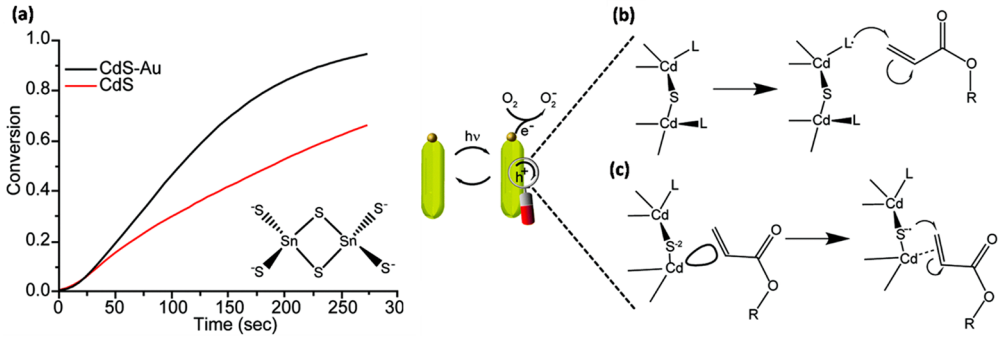

Figure 6. (a) Conversion of HEA monomers versus time. Polymerization photoinitiated by $Sn_2S_6^{4-}$-coated bare NPs (red) and HNPs (black). (b) Proposed mechanism 1: charge transfer via surface coating mediation. (c) Proposed mechanism 2: charge transfer via anion-localized state. Adapted with permission from ref 71. Copyright 2019 Royal Society of Chemistry.

with an electron-deficient lead (Pb) site on the perovskite surface, giving rise to an active radical under irradiation and triggering a chain propagation process. Termination of polymerization could happen through the combination of propagating radicals or chain transfer, and the polymer might still attach to the NCs' surface after the reaction. High molecular weight polymers of around 200 kDa, dispersity around 2.0, and conversion over 12% were obtained after 14 h illumination. The free-radical chain-growth polymerization mechanism was also evidenced by a total restraint of polymerization in the presence of radical inhibitors.

Banin and co-workers recently developed a CdS−Au hybrid NP-photoinitiated solvent-free polymerization through a surface charge transfer mechanism.[71] Without any additives, inorganic ligand $Sn_2S_6^{4-}$-capped hybrid NPs could initiate the photopolymerization of hydroxyethyl acrylates (HEA), achieving almost full conversion within 300 s, showing efficiency higher than that of the bare CdS (Figure 6a). Two possible surface initiation mechanisms were proposed. The authors suggested, in the first pathway, charge transfer between excited HNPs and monomers could happen via surface coating/ligand mediation, where surface ligands could act as hole traps/acceptors to transfer the excited holes to the monomers (Figure 6b). The second pathway involved an interaction between the excited NPs and double bonds on monomers, followed by a charge transfer from the anion-localized surface of NPs to monomers (Figure 6c). Although further investigations are still needed, the surface-induced initiation mechanism provides a cornerstone for future study.

4.2. Living/Controlled Radical Polymerizations (CRPs) Photoinduced by SNMs

In this section, we explicitly highlight the current developed SNMs for mediating photo-CRPs, particularly for ATRP and RAFT polymerization.

4.2.1. Photoinduced ATRP Catalyzed by SNMs. For traditional ATRP, the reversible activation/deactivation process highly depends on the redox cycle of Cu(I)/Cu(II).[6,62,89] Introducing photosensitizers such as SNMs into polymerization systems appear to be a promising way to mediate the equilibrium of Cu(I)/Cu(II) species and achieve a high degree of photocontrol. Indeed, graphitic carbon nitride,[166] carbon QDs,[144] TiO_2NPs,[167] ZnO/Fe-doped ZnO NPs,[88] and titania/reduced graphene oxide nanocomposites[168] have been reported to work as photosensitizers in copper-mediated ATRP. The photoexcited SNMs could reduce the copper catalysts from Cu(II) to Cu(I), and the resulting Cu(I)-active species could further react with alkyl halides and return back to the high valence state, while reduced alkyl radicals initiate the ATRP process (Figure 7a). In general, a

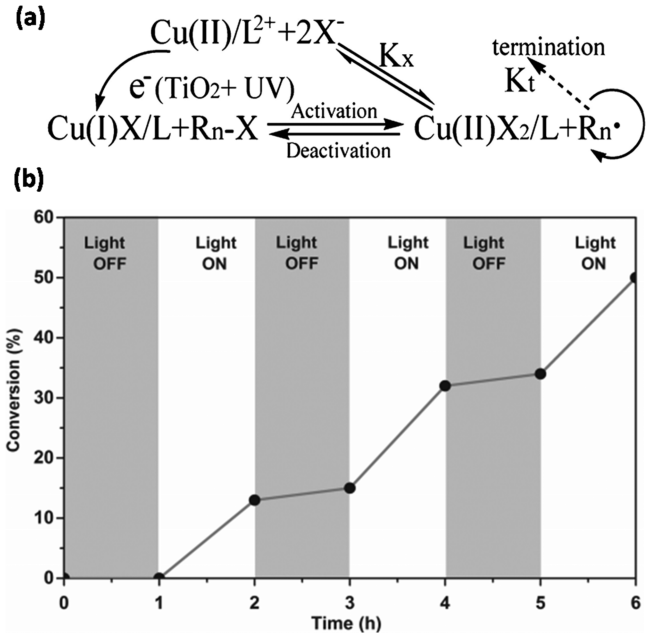

Figure 7. (a) Proposed mechanism of UV-light-induced ATRP polymerization using NMs (TiO_2). Adapted from ref 167. Copyright 2013 American Chemical Society. (b) Monomer conversion versus time when light is "on" and "off". Adapted with permission from ref 88. Copyright 2014 John Wiley and Sons.

good correlation between experimental and theoretical molecular weights was observed in the all of the above cases, and a variety of monomers including methacrylates[88,144,167] and acrylamides[167] were successfully polymerized through SNM-photosensitized ATRP. However, UV light was used as the primary irradiation source,[88,166,167] which requires high energy consumption and might lead to the monomer self-initiation.[169] Moreover, temporal control could not completely be achieved in some cases, which might be because of the residual Cu(I) catalyst after photoactivation.[92] For example, when ZnO was used as the photosensitizers for Cu(II)Br_2-mediated polymerization of MMA,[88] the monomer conversion still slightly increased even when the light was "off" (Figure 7b).

https://doi.org/10.1021/acspolymersau.1c00014
ACS Polym. Au 2021, 1, 76−99

In 2015, Liu's group reported a copper-free photoinitiated ATRP using niobium (Nb) NPs as a new class of recyclable PCs in the presence of ethyl 2-bromoisobutyrate (EBiB) initiators.[170] The resulting polymer showcased low dispersity ranging from 1.16 to 1.30 and controlled molecular weights. EBiB was proposed to be activated by the carbon-centered radical on the benzyl alcohol ligand originated from photo-induced ligand to metal charge transfer. However, chain extension was not performed in this study to explore the chain end fidelity of the resulting products.

Apart from serving as photosensitizers, SNMs could also work as PCs for ATRP. In 2018, Egap's group reported the very first example of visible-light-mediated ATRP polymerization using CdSe QDs as PCs.[93] A wide variety of functional monomers (Figure 8a) were successfully polymerized with

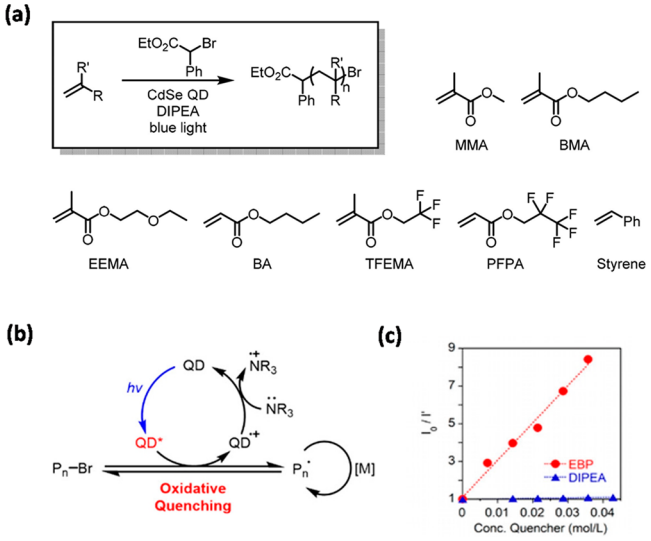

Figure 8. (a) Monomers and (b) proposed mechanisms of photo-ATRP polymerization catalyzed by CdSe QDs. (c) Stern–Volmer plot of CdSe QD fluorescence quenched by EBP and DIPEA. Adapted from ref 93. Copyright 2018 American Chemical Society.

high yield (48.3–99.0%) and moderate dispersity ($Đ$ = 1.25–1.83) using 3.3 nm CdSe QDs in the presence of external sacrificial donor *N*,*N*-diisopropylethylamine (DIPEA). Due to the sufficiently negative reduction potential of CdSe QDs (−1.59 vs SCE)[111] and large absorption coefficient efficiency[117] (over 10^6 M^{-1} cm^{-1}), polymerization could be conducted in the presence of only 0.4 mM catalyst concentration. Excellent spatial and temporal control of the polymer architectures was achieved, and block copolymer was obtained via macroinitiator chain extension, indicating the strong living characteristic of the polymerization. A TEA-assisted oxidative quenching cycle was proposed to describe the mechanism (Figure 8b). First, excited-state QDs* were generated under irradiation and subsequently reduced the dormant bromide chain end to a radical under irradiation, which then participated in propagating monomers. The QD radical cation forming from the PET process could then accept an electron from DIPEA to complete the catalyst cycle. A Stern–Volmer plot of CdSe QDs PL quenching at various concentrations of alkyl bromide initiators or DIPEA showed that initiators are far more effective than DIPEA in quenching the PL of CdSe (Figure 8c), suggesting alkyl bromide was more likely to react with excited QDs. However, one drawback of this polymerization system is that the amine radical anion intermediate forming from catalyst step turnover[28,158] could probably end-cap the radicals and lead to undesirable termination.[28] Moreover, due to nonpolar ligand capping on CdSe QDs, polymerization could not be operated in polar solvents, which are known for facilitating electron transfer and stabilizing charge-separated species.[171]

4.2.2. Photoinduced RAFT Polymerization Catalyzed by SNMs. An essential factor to achieve a successful RAFT polymerization is utilizing an appropriate amount of external initiation species such as azobisisobutyronitrile to initiate chain transfer agents.[172] SNM photoinitiators, which could efficiently produce active radicals under photoexcited states, appear to be good candidates for RAFT polymerization initiation. In 2014, Liu's group developed a well-controlled visible-light-mediated RAFT polymerization enabled by surface-modified Nb-$(OH)_5$NPs.[173] The authors proposed a photoinitiated RAFT polymerization mechanism[42,174,175] where excited electrons could transfer from surface ligands to the metal atom core, forming a radical cation at the surface (Figure 9a). The radical cation then lost one α-hydrogen, giving rise to a −O−CH−Ph radical, which further attacked the RAFT agent and started the RAFT process. Small dispersity ($Đ$ = 1.17) could still be achieved even at 86% monomer conversion, where chain termination and side reactions often happen at such high conversion. Polymerization could be started or stopped at will simply by turning the light on and off, and dormant species were still able to be activated even after six cycles of the light "on–off" (Figure 9b). As no polymerization was observed without $Nb(OH)_5$ NPs, the ability to control the activity of polymerization is due to the incorporation of SNMs rather than the photolysis of RAFT agents. NPs could be recovered from the reaction mixture and still efficiently initiate the RAFT polymerization, giving more than 70% monomer conversion even after six recycle times. However, polymer yield gradually decreased and $Đ$ increased after every recycle (Figure 9c), which is probably due to partially losing grafted groups on the NP surface.[173]

One of the challenges in photoinitiated RAFT polymerization is that the use of co-initiating radicals might cause undesired chain termination.[2] On the other hand, directly reducing RAFT agents using PCs could circumvent the formation of initiator-derived byproducts and meanwhile maintain the temporal control over polymerization.[2,8] Very recently, CdSe QDs were proven to be robust PCs for PET-RAFT polymerization in both organic[176,177] and aqueous[178] solutions. CdSe QDs have a strong reducing potential (−1.59 vs SCE for 3.3 nm QDs), which is sufficient to reduce typical RAFT agents (redox potential ranging from −0.3 to −0.8 V vs SCE). In 2019, Egap's group[176] demonstrated an efficient PET-RAFT polymerization in various polar organic solvents including dimethylsulfoxide (DMSO), *N*,*N*-dimethylacetamide, and *N*,*N*-dimethylformamide (DMF). A broad scope of functional methacrylate and acrylate monomers was successfully polymerized, with $Đ$ ranging from 1.09 to 1.24. The di- and trithio-CTAs were found to bind with the metal core of CdSe QDs surface via Lewis acid–base interaction[179] and partially substitute the original ligands, thus allowing in situ growth of polymer chains from the surface of CdSe QDs to form well-dispersed core–shell polymer–QD nanocomposites (Figure 10a). Weiss' group[178] reported an aqueous PET-RAFT polymerization of a series of acrylamides and acrylates using CdSe QDs as PCs. The polymerization could be operated

https://doi.org/10.1021/acspolymersau.1c00014
ACS Polym. Au 2021, 1, 76–99

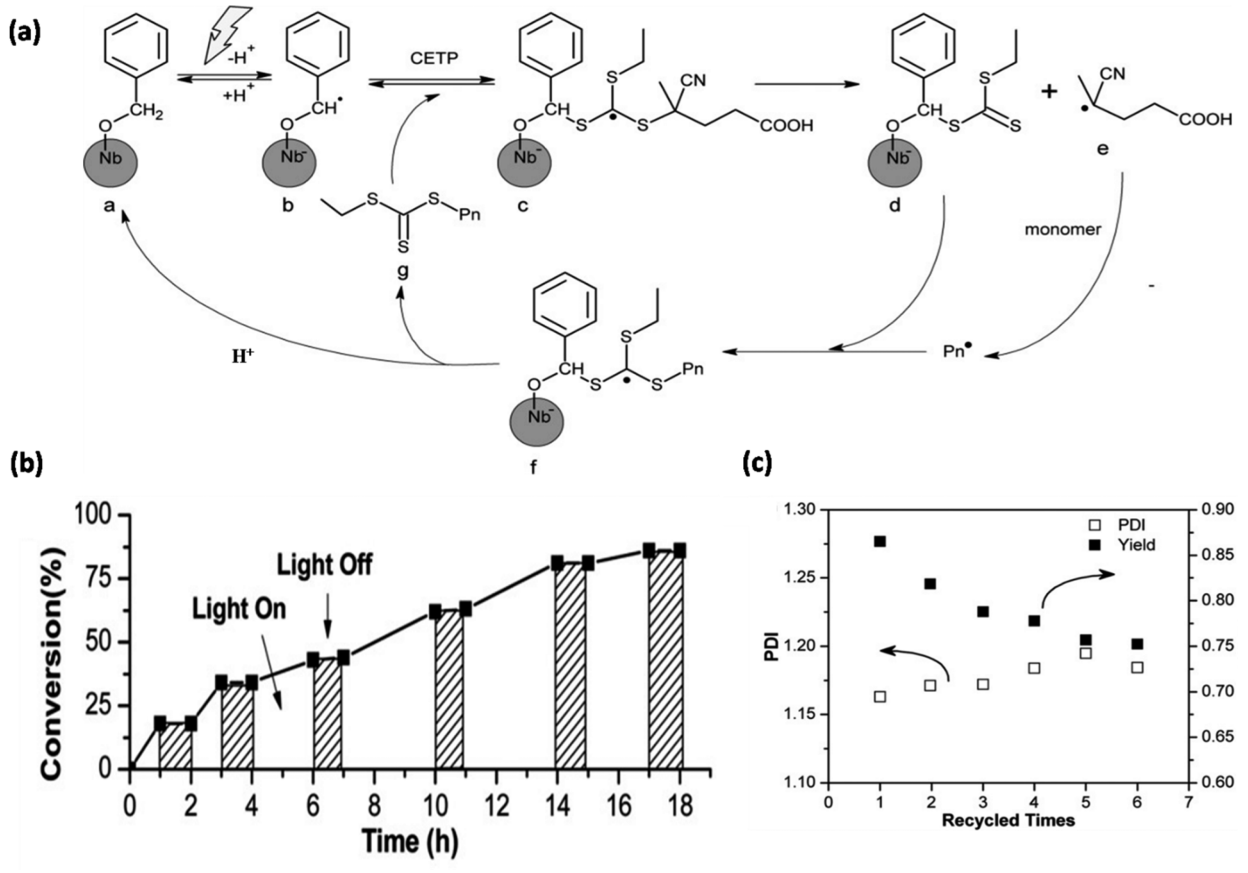

Figure 9. Photoinitiated RAFT polymerization triggered by $Nb(OH)_5$ NPs. (a) Proposed mechanism. (b) Monomer conversion versus time while turning the light on and off. (c) $Đ$ and yields of polymer versus recycle times. Adapted with permission from ref 173. Copyright 2014 John Wiley and Sons.

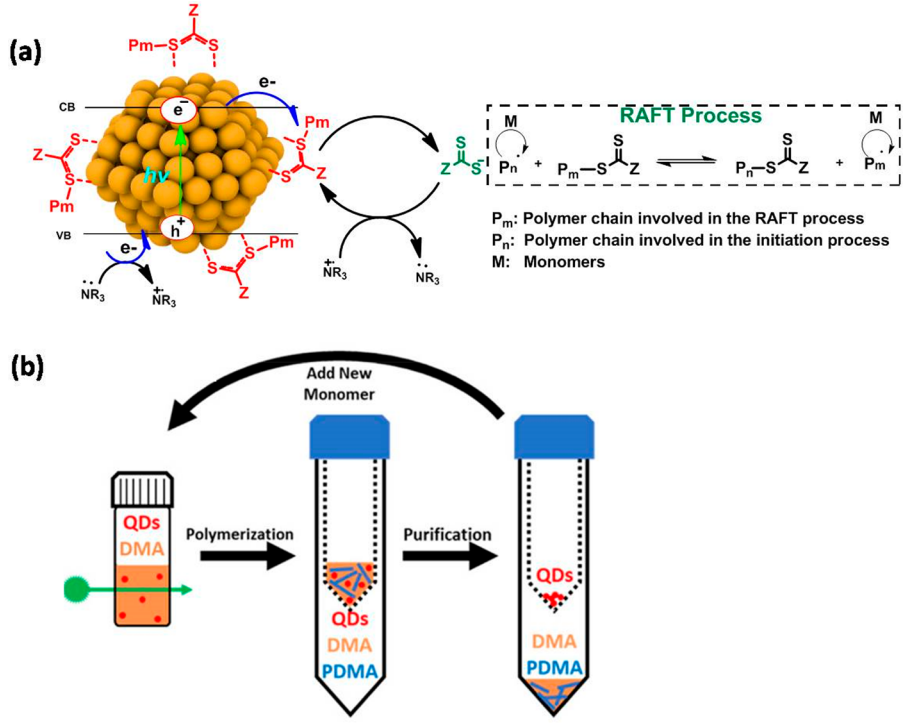

Figure 10. (a) Proposed mechanism of CdSe QD-catalyzed PET-RAFT polymerization in organic solvents and in situ growth of the polymer shell. Adapted with permission from ref 176. Copyright 2020 Royal Society of Chemistry. (b) Procedure for the separation of QDs from polymer products. Adapted from ref 178. Copyright 2020 American Chemical Society.

https://doi.org/10.1021/acspolymersau.1c00014
ACS Polym. Au 2021, 1, 76−99

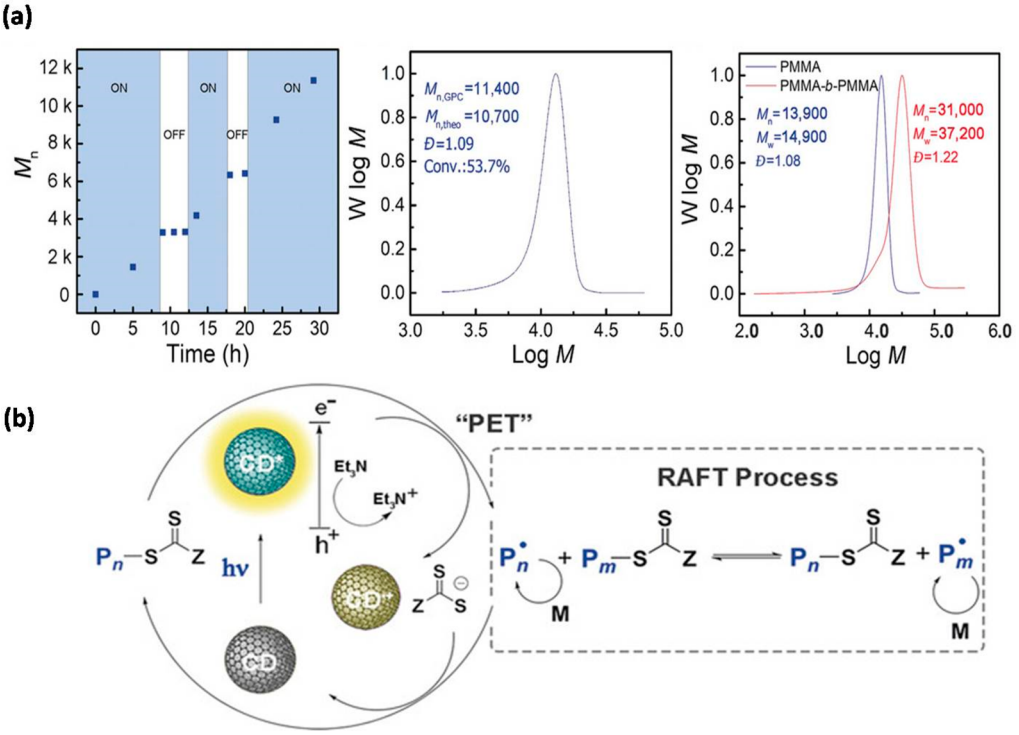

Figure 11. (a) Light "on/off" experiments catalyzed by CDs (left), GPC profile of the PMMA (middle), and GPC profiles of PMMA macroinitiator and the diblock copolymer after chain extension (right). (b) Proposed mechanism of CD-photocatalyzed RAFT polymerization. Adapted with permission from ref 103. Copyright 2018 John Wiley and Sons.

under ultralow (<0.5 ppm) QD loadings, resulting in more than 90% monomer conversion in 2.5 h and low dispersity (<1.10). Furthermore, using protein concentrators with large-pore (30 kDa) filters (Figure 10b), polymers could be isolated and QDs could selectively be retained in the concentrate. Moreover, the size effect of CdSe QDs over the RAFT polymerization has also been recently reported by Pang's group.[177] The better controllability of polymerization was observed using larger-size QDs (6.8 nm) than using the 3.8 nm QDs.

Although CdSe QDs have shown excellent catalytic performance in photomediated RAFT polymerization, the residual toxic metal Cd raises the concern of contamination of the polymer products. Therefore, utilizing metal-free SNMs such as carbon QDs,[103,180] silicon quantum dots,[181] nanofibers,[146] and nanosize-conducting polymers[145] becomes an alterative approach for PET-RAFT polymerization. For example, Matyjaszewski and co-workers developed a robust metal-free PET-RAFT polymerization using heteroatom-doped carbon quantum dots (CDs) as a new class of PCs.[103] Well-defined polymers with corresponding molecular weights and small dispersity ($Đ$ < 1.10) could be obtained from this approach under blue light-emitting diodes and natural sunlight. Formidable control over the polymerization process was revealed by excellent spatial control (Figure 11a, left), monomodal and symmetric GPC profiles (Figure 11a, middle), as well as successful chain extension (Figure 11a, right). The authors found that doping the heteroatom could promote the polymerization efficiency, and further screening different heteroatoms showed that P- and S-doped CDs were more effective PCs, likely due to their strong absorption in the blue light region and high degree of graphitization. A typical PET-RAFT polymerization mechanism via an oxidative quenching pathway was proposed (Figure 11b), and the authors also found that introducing sacrificial hole scavengers would increase the excited CD lifetimes by preventing charge recombination and therefore would enhance the overall polymerization efficiency.

Metal oxide NPs have also proven to be efficient PCs for RAFT polymerization. Nano-ZnO (30 nm) was developed by He and co-workers as a PC for PET-RAFT polymerization of MMA in DMF at ambient temperature.[182] UV light was used as the irradiation source due to the ZnO absorption spectrum, achieving around 15% of monomer conversion and $Đ$ > 1.40 for 5 h. A similar strategy for PET-RAFT polymerization was reported by You and co-workers using TiO_2 (type P25) as a photoredox catalyst under UV light.[183] It is worthwhile to mention that the photolysis of RAFT agents is likely to happen under UV irradiation,[90] where RAFT agents could be directly photoinitiated and propagate with monomers. Therefore, the photolysis process may occur in parallel with PET-RAFT polymerization using ZnO and TiO_2 NPs with UV light. A control study without metal oxide NPs could be useful to distinguish two different polymerization pathways.

One of the major challenges in the aforementioned PET-RAFT polymerization is that the irradiation wavelength is limited to the blue and UV light regions. The high energy light not only may lead to undesired photolysis of RAFT agents[184,185] but also may not be cost-effective due to the high energy consumption. Therefore, the development of PCs upon far-red and near-infrared (NIR) irradiation for photoinduced polymerization is of general interest.[76,169,186,187] In 2020, Egap's group reported lead halide perovskite ($CsPbBr_3$) NCs as band-edge-tunable PCs for efficient photoinduced visible and NIR irradiation.[54] By simply modulating the ratio of iodine and bromine in the $CsPbBr_xI_{3-x}$ NCs, the perovskite-

https://doi.org/10.1021/acspolymersau.1c00014
ACS Polym. Au 2021, 1, 76−99

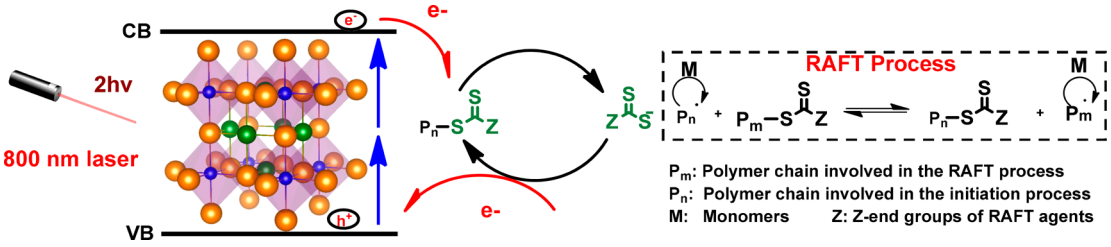

Figure 12. $CsPbBr_3$ NC-photocatalyzed RAFT polymerization via two-photon absorption. Adapted from ref 54. Copyright 2020 American Chemical Society.

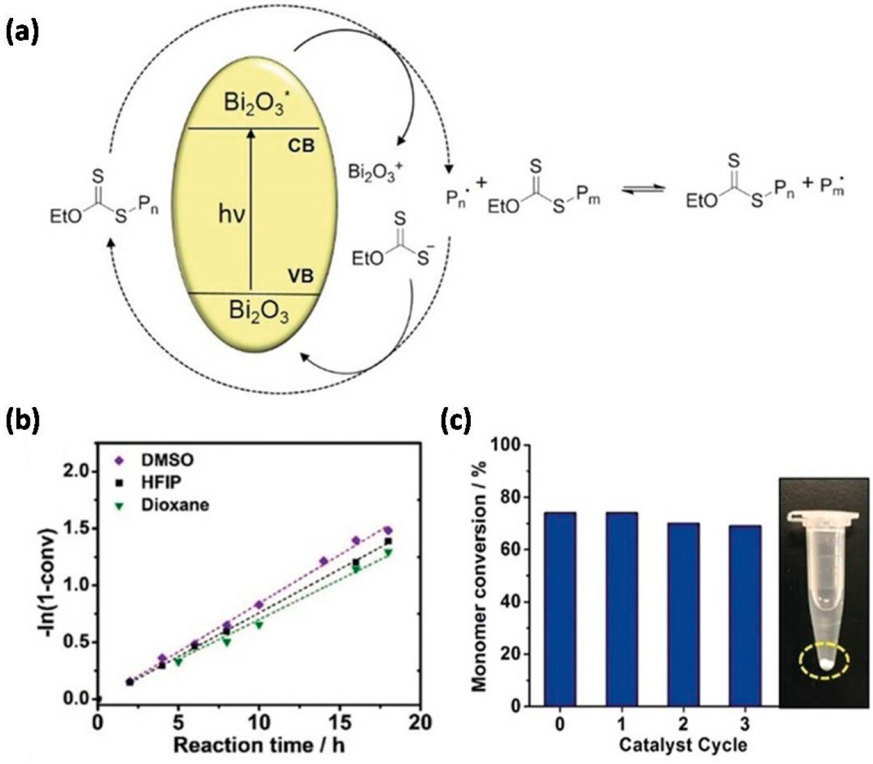

Figure 13. (a) MADIX/RAFT polymerization photomediated by Bi_2O_3. (b) Kinetic plot of the MADIX/RAFT polymerization in different solvents. (c) Recycling of the Bi_2O_3 catalyst and polymerization effect. Adapted with permission from ref 95. Copyright 2019 John Wiley and Sons.

catalyzed PET-RAFT polymerization of various functional acrylates and methyacrylates could be performed under a broad range of irradiation sources ranging from blue to red light (460−635 nm), yielding polymers with small dispersity ($Đ$ = 1.02−1.13). More importantly, by leveraging the extremely large two-photon absorption (TPA) cross section of $CsPbBr_3$ (1.8×10^5 GM), the authors performed a TPA-induced PET-RAFT polymerization with irradiation of an 800 nm laser. $CsPbBr_3$ was proposed to simultaneously absorb two 1.55 eV photons, giving one above-gap excitation and transferring excited electrons to RAFT agents (Figure 12). Encouragingly, the polymerization was conducted in a controlled fashion, achieving 60.2% monomer conversion and $Đ$ = 1.07. The TPA-induced RAFT polymerization demonstrates the great potential of SNMs as NIR PCs for photopolymerizations.

Apart from the aforementioned nanostructures, microsized semiconducting materials such as graphitic carbon nitride (g-C_3N_4)[147] and bismuth oxide (Bi_2O_3)[95] were also introduced recently as reusable and recyclable PCs for PET-RAFT polymerization. In the case of g-C_3N_4, the robust catalytic nature was revealed by successfully conducting polymerization with nonpurified monomers and air, providing various opportunities for large-scale industrial applications.[42] Bi_2O_3, on the other hand, was reported to mediate a macromolecular design by the interchange of xanthate (MADIX)/RAFT polymerization for both more activated monomers and less activated monomers using only a general household light bulb (Figure 13a). Polymerization could be operated in a variety of solvents including DMSO, hexafluoroisopropanol, and dioxane (Figure 13b) with a pseudo-first-order kinetics feature, offering polymers with precise control over MW and small dispersity less than 1.20. In addition, heterogeneous Bi_2O_3 could be removed from the reaction mixture and reused for at least three cycles with a negligible reduction in catalytic performance (Figure 13c).

In 2020, Müllner's group reported a facile method to incorporate alkyl bromide redox chemistry into the RAFT process using Bi_2O_3 as the PC.[110] Alkyl bromides were proposed to be reduced by photoexcited Bi_2O_3 and generating an active radical. The alkyl radicals could react with RAFT agents and promote a controlled photopolymerization. The

https://doi.org/10.1021/acspolymersau.1c00014
ACS Polym. Au 2021, 1, 76−99

presence of the alkyl substituent and trithiocarbonate from RAFT agents was further confirmed by nuclear magnetic resonance and electrospray ionization mass spectrometry. The control of polymerization was governed by the degenerative chain transfer process onto RAFT agents rather than the alkyl bromide redox equilibrium. A wide variety of functionalities including peptides could be installed into polymer using different alkyl bromides. Furthermore, varying the ratio of two different RAFT agents in the reaction mixture could tune the dispersity of resulting polymers from 1.18 to 1.64.

4.3. Other Types of Polymerization Photoinduced by SNMs

We summarized herein other types of photopolymerization mechanisms induced by SNMs apart from chain-growth radical mechanism. For instance, Ravoo's group reported a step-growth polymerization of ethanol amines driven by TiO_2 NPs upon UV irradiation to prepare microstructured polymer brushes.[188] The authors suggested that ethanol amine monomers could accept photogenerated holes from TiO_2 NPs, forming the corresponding aldehyde that reacted with another ethanol amine molecule to yield imine. Imines were then reduced to secondary amines by photoexcited electrons in the CB of TiO_2 to complete the catalytic cycle.

Conjugated polymers have received great interest due to their wide application in fabricating various materials such as optoelectronic devices[189] and batteries.[190] The mechanism of photoinduced polymerization of conjugated polymers usually begins with hole transfer from photosensitizer to monomer followed by the monomer radical cation coupling.[191] We herein highlight the photoinduced methodology for synthesizing conjugated polymers using NMs, a technique that is rarely reported but possesses great potential. For example, Neckers and co-workers reported a photopolymerization of oligothiophene-decorated Au NPs.[192] 5-Mercapto-2,2′-bithiophene (BTSH) was attached to the Au NPs' surface through thiol–gold bonds. Upon UV irradiation, bithiophene was able to be oxidized by Au NPs, which have a strong electron affinity, via intramolecular electron-transfer reactions. The oxidized radical cation rapidly coupled with other bithiophene radical cations, leading to the formation of polythiophene and aggregation of Au NPs. The photopolymerization among Au NPs was further confirmed by UV absorption spectrum of Au NPs after irradiation, where the plasmon absorption band was broadened and red-shifted. Furthermore, femtosecond transient absorption showcased that charge separation rates between bithiophene ligands and Au NPs decreased with increasing NP sizes.

Bulk materials such as TiO_2 were also examined to polymerize pyrrole[193] and 3,4-ethylenedioxythiophene[194] in situ at their surface, which would form a conducting polymer layer. Electrophiles such as F-SnO_2 electrodes or oxygen were used to accept photoexcited electrons, whereas monomers react with surface-trapped holes, giving rise to the conducting polymer layer via the radical coupling. The formation of conjugated polymers was supported by FTIR spectroscopy and cyclic voltammetry results. Moreover, Ag NPs have also been reported to polymerize pyrrole via a similar mechanism.[195,196] However, these reports lack of comprehensive study on reaction yield, MW, as well as dispersity.

Recently, Tüysüz reported a photoinduced polymerization of synthesizing poly(3,4-ethylenedioxythiophene) (PEDOT), enabled by cesium lead iodide ($CsPbI_3$) perovskite QDs (Scheme 4).[135] Because the oxidation potential of 3,4-ethylenedioxythiophene (1.9 V vs NHE) is energetically lower than the VB of $CsPbI_3$ QDs (1.3 V vs NHE), the direct reduction of 3,4-ethylenedioxythiophene is energetically unfavorable. Thus, trimer 3,4-ethylenedioxythiophene (TerEDOT), whose oxidation potential located at 0.8 V vs NHE, was used instead as the starting monomer. Successful polymerization of TerEDOT was confirmed by the appearance of a broad peak around 750 nm in the UV absorption spectrum, and TEM images displayed that $CsPbI_3$ QDs were encapsulated into the polymer matrix. Furthermore, because oxygen could be used as electron acceptors for $CsPbI_3$ QDs, polymerization could be performed in air. However, the crystal structure of $CsPbI_3$ QDs transformed from cubic to orthorhombic after reacting in air. The change of crystal structure might be induced by the oxidation and removal of surfactants on the QDs. A recent study by Chen's group[137] revealed that the polymerization efficiency of TerEDOT could be highly enhanced by simply treating $CsPbI_3$ QDs with methyl acetate. The use of methyl acetate could replace the original oleic acid ligands and introduce defects on the surface of QDs, which might accelerate the charge transfer and impede the radiative charge recombination.

Scheme 4. Proposed Mechanism for Polymerization of TerEDOT Using $CsPbI_3$ QDs as PCs[a]

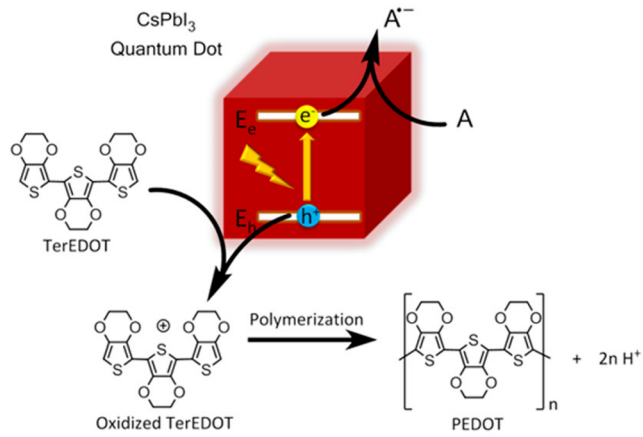

[a]Adapted from ref 135. Copyright 2017 American Chemical Society.

5. APPLICATION OF NM-INDUCED PHOTOPOLYMERIZATION

5.1. Photoinduced Three-Dimensional (3D) Printing Using NPs as PIs

Photopolymerization-based 3D printing has attracted significant attention from both academic and industrial research in recent years.[197,198] This rapidly developing technology offers a facile route for fabricating functional materials with various optical, chemical, and mechanical properties.[197,199] A representative 3D printing system is composed of monomers, oligomers, and PIs. Beginning with the liquid state monomers/oligomers, PIs can be activated upon exposure to the light source and triggered a cured/photopolymerized process, leading to the solidification of liquid monomers. To achieve successful photopolymerization, the polymerization/cross-linking process should be fast enough (typically reaching full conversion in 1 min)[197] so that the ink could be rapidly

https://doi.org/10.1021/acspolymersau.1c00014
ACS Polym. Au 2021, 1, 76–99

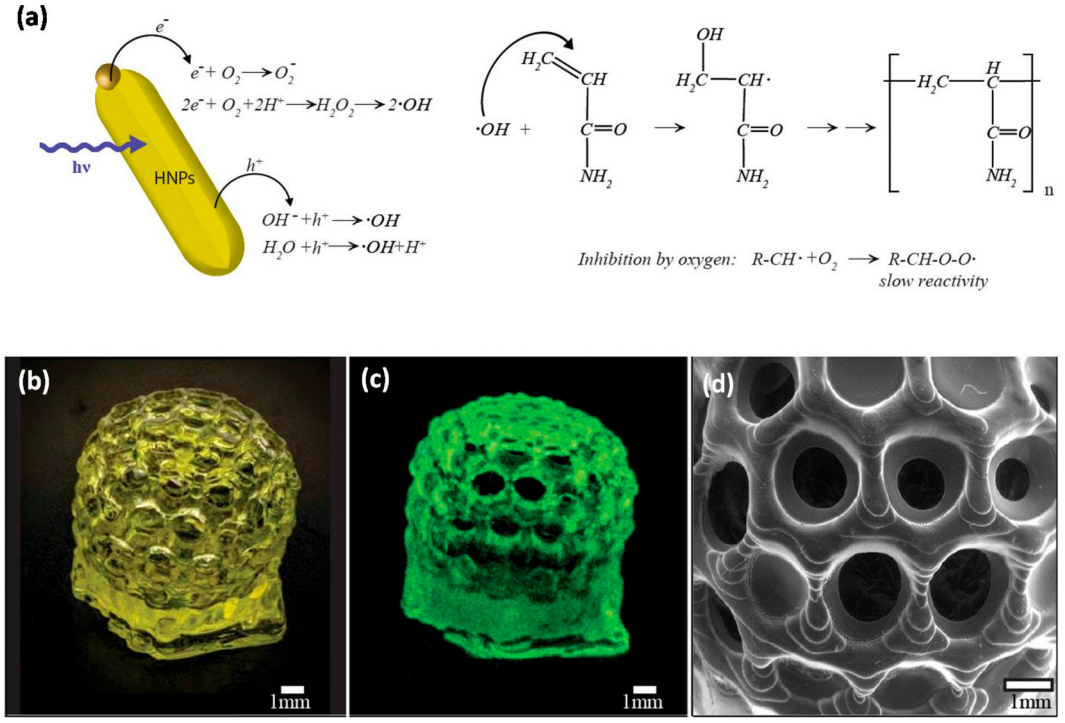

Figure 14. (a) Mechanism of polymerization using CdS−Au HNPs as photoinitiators. (b) Images of a 3D-printed buckyball under regular light and (c) under 365 nm excitation. (d) Scanning electron microscopy image of the dried structure. Adapted from ref 85. Copyright 2017 American Chemical Society.

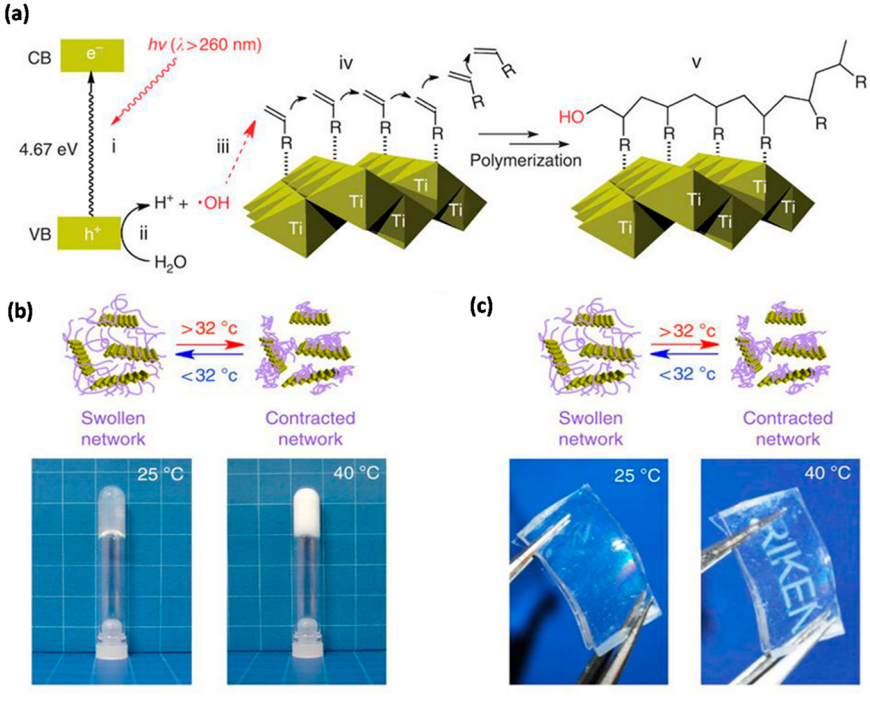

Figure 15. (a) In situ photoinduced polymerization and formation of nanocomposite hydrogelation catalyzed by TiNSs. (b) Formed thermal responsable hydrogel under different temperatures in test tubes and (c) in a patterned matrix. Adapted with permission from ref 208. Copyright 2013 Springer Nature.

transformed into the solid state.[198] Due to the large absorption coefficient, SNM-photoinduced polymerization provides new opportunities for conducting photo-3D printing under low catalyst loading.[123] The easily tunable solubility of SNMs even enables the photo-3D in the aqueous phase.[200]

In 2017, Magdassi and Banin reported a rapid water-phase 3D printing using hybrid semiconductor−metal NPs as a novel class of PIs (Figure 14a).[85] Excited electron−hole pairs origin from CdS/Au HNPs were proposed to react with water and oxygen, producing hydroxyl and superoxide radicals to initiate

https://doi.org/10.1021/acspolymersau.1c00014
ACS Polym. Au 2021, 1, 76−99

polymerization, and meanwhile HNPs could remain intact. This highly efficient polymerization was used for 3D printing of hydrogels by a digital light projector printer with UV light, giving rise to a spherical C180 buckyball hydrogel object (Figure 14b). Polymerization also showed good oxygen tolerance, and the printing process could be operated in the presence of only 0.2 nM HNPs. The 3D-printed buckyball hydrogel also exhibited strong green fluorescence under 365 nm excitation (Figure 14c), retaining delicate structures even after drying (Figure 14d).

Magdassi also established a rapid 3D printing method for fabricating complex hydrogels with UV-curable inks.[200] 2,4,6-Trimethylbenzoyldiphenylphosphine oxide (TPO) was converted into water-dispersible NPs and used as the PIs, enabling building a stable woodpile-structured hydrogel within 25 min. TPO also showcased the superior performance in 3D printing over other common organic dye PIs under identical conditions. The excellent polymerization performance facilitated by TPO NPs was attributed to the good solubility and dispersion of the TPO in water.

5.2. Synthesis of Organic–Inorganic Nanocomposites via In Situ Photopolymerization

Polymer nanocomposites are a class of advanced materials that have been widely used in optical/electrical sensors,[201] batteries,[202,203] light-emitting diodes,[204] absorption,[205,206] and biological imaging.[207] With SNMs as photomediators, SNM-photoinduced polymerization emerges as a novel strategy to fabricate organic–inorganic nanocomposites.

In 2013, Aida and co-workers developed a facile synthesis method of photomodulable thermoresponsive hydrogels photocatalyzed by titania nanosheets (TiNSs).[208] Upon irradiation, TiNSs produced hydroxyl radicals from water, which initiated polymerization and meanwhile cross-linked the polymer chains to form a 3D polymer network (Figure 15a), which could hold the water molecules. Various water-soluble vinyl monomers including acrylamide and *N*-isopropylacrylamide underwent such a gelation process. The yielded hydrogels showed sharp thermoresponses (Figure 15b,c) and an excellent resolution on pointwise modulations. A similar strategy was also employed for temperature-responsive poly(*N*-isopropylacrylamide) hydrogel using carbon nitride nanosheets (CNNs) as PCs.[209] The hydroxyl radicals from water generated on CNNs were claimed as the initiating species. The nanocomposites could act as a temperature-controlled smart window around the lower critical solution temperature, reversibly altering the turbidity. This in situ polymerization/cross-linking route offers a facile synthesis of functional carbon nitride composite hydrogels with a promoted photocatalytic performance in removing organic pollutants, strong mechanical properties, and adjustable shapes.[210−212]

Wang and Wu also demonstrated the synthesis of nanoparticle–hydrogel composites with the aid of semiconductor NPs and clay nanosheets.[213] NPs were used for generating initiating hydroxyl radicals under sunlight, and clay nanosheets were utilized for increasing cross-linking points, as the cross-linking points on the NP surfaces were insufficient. Various NPs including zinc oxide, titanium dioxide, iron(III) oxide, tin dioxide, zirconium dioxide, cadmium selenide, or cadmium telluride were established for successful photoinitiated polymerization of *N*,*N*-dimethylacrylamide. Formed nanocomposite hydrogels exhibit high toughness and elasticity (Figure 16a), and all of the hydrogels could tolerate a compression greater than 95%. The physicochemical properties of the semiconductor NPs were remained after polymerization, providing hydrogels with different fluorescence wavelengths via simply changing the size of the QDs (Figure 16b).

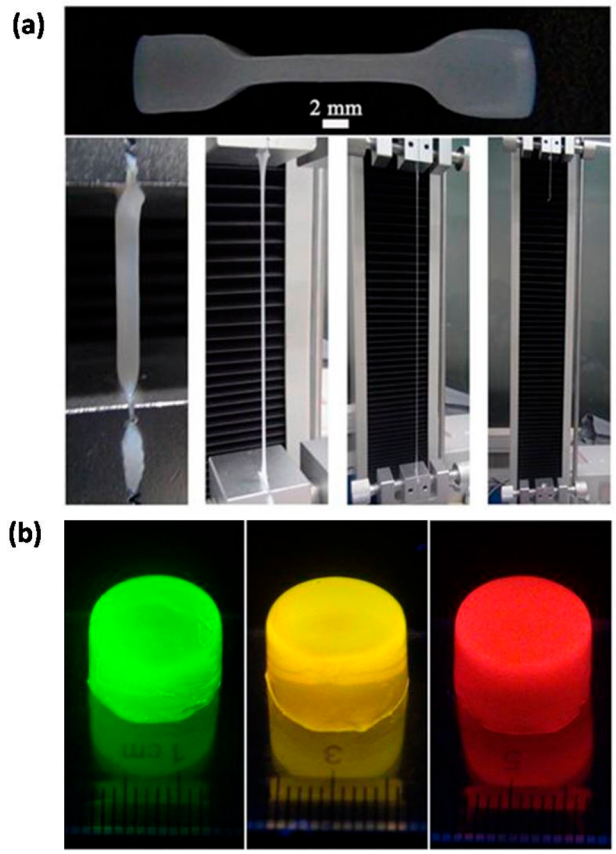

Figure 16. (a) Images of the NC hydrogels during the tensile testing process. (b) Images of different fluorescence CdTe-NC hydrogels under UV light. Adapted with permission from ref 213. Copyright 2013 Springer Nature.

Very recently, Acar and co-workers fabricated luminescent ZnO/MMA nanocomposites utilizing methacrylic-acid-coated ZnO QDs as the photoinitiator.[214] Starting with Kolbe decarboxylation of surface-coated carboxylic acids by photoexcited ZnO, successful photopolymerization of MMA was performed in bulk and methylethyl ketone, giving rise to a homogeneous gel with strong yellow luminescence. No luminescence of ZnO was quenched during the polymerization. The same group also reported a facile method to form luminescent and stable CdS QD/polymer hybrids via the decarboxylation process of the oleic acid ligand.[215]

Although the aforementioned examples could incorporate SNMs into the polymer matrix, incompatibility between inorganic nanobuilding blocks and organic polymers usually leads to phase separation and aggregation of SNMs.[176,216] On the other hand, the direct growth of polymers on the surface of SNMs ("grafting from") enables both the polymer matrix and the shell of nanobuilding block to have the same chemical structure and hence to be miscible with each other.[176,217] By modifying the surface of photoactivated SNMs with initiation species, the SNMs could serve as both the PCs and inorganic nanocomposites, enabling the photopolymerization to happen in situ on the SNMs' surface and forming well-dispersed polymer–SNM nanocomposites.[167,218,219] We also believe that

https://doi.org/10.1021/acspolymersau.1c00014
ACS Polym. Au 2021, 1, 76−99

shortening the distance between SNMs and initiators would enhance the electron transfer rate by increasing the collision frequency,[220] consequently speeding up the rate of polymerization. For example, Yin and co-workers established a facile synthesis of inorganic−polymer hybrid nanocomposites using TiO_2 nanospheres as PIs (Figure 17a).[218] The TiO_2 NP surface was modified by 3-(trimethoxysilyl)propyl methacrylate (MPS) as the Si−O−Ti linkages. MPS moieties accepted the photogenerated radicals on the NPs' surface, serving as initiators, and continuously propagated polymers, coating the polymer on the NPs' surface uniformly, even in the presence of oxygen. TEM images showcased the successful formation of polymer shells on the NPs' surface (Figure 17b). Faster polymerization was observed with higher crystallinity of the titania nanospheres. This technique could be generalized to other core materials such as SiO_2 and ZnS by simply coating the substrates with the TiO_2 thin layer.

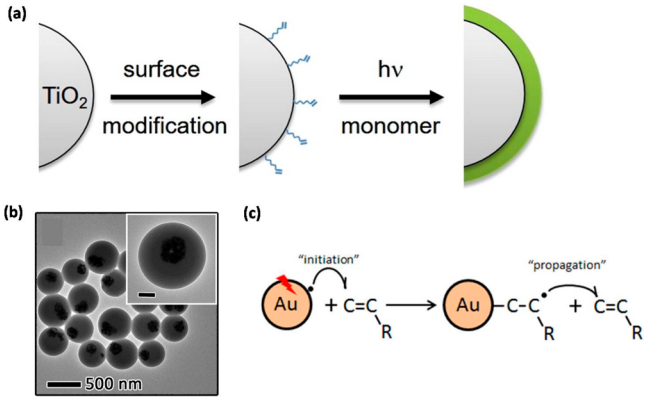

Figure 17. (a) Schematic illustration of surface-initiated polymerization using TiO_2 as PC and building block core for polymer grafted NPs. (b) TEM image of polymer grafted TiO_2 NPs. Panels (a) and (b) are adapted from ref 218. Copyright 2016 American Chemical Society. (c) Hot electron initiated photopolymerization. Adapted from ref 73. Copyright 2017 American Chemical Society.

Very recently, plasmon-induced polymerization appears to be an alternative method to coat polymer on the surface of the nanostructures.[73,75,221] Monomers are usually initiated by injection of hot electrons photogenerated by plasmons. Hot-electron initiation occurs close to the metal NPs (Au, Ag, etc.) surface, enabling polymerization happening within the nanogap. Monomers are initiated through the formation of [metal−C−C•] species near the NPs' surface (Figure 17c). Nobel metal NPs, such as Au and Ag, were used as the nanobuilding block, and a blue shift of the plasmon resonances was usually observed after polymerization.[73] A large scope of vinyl monomers with different functional groups and conjugated polymers[222] can be produced via this methodology. More importantly, by changing the position of the hotspots, hot electron injection density can be optimized, leading to the growth control of the polymer shell. The plasmon-induced mechanism is also applied for controlled polymerizations such as NMP[223] and RAFT[76,224] polymerization. Although surface modification of covalently attaching initiators on the gold particle surface was required, the living polymerization allowed the grafting block copolymers on the metal surface and control over polymer shell thickness.

6. CONCLUSION AND FUTURE OUTLOOK

Utilizing SNMs as PIs/PCs has blossomed into an attractive field due to the recent resurgence of interest in photoinduced polymerization. Compared to currently developed metal complexes and organic PIs/PCs, SNMs provide added advantages such as simple synthesis procedures, abundant raw materials, and tunable band gaps and redox potentials. Various SNMs including metal oxides, metal chalcogenide QDs, and perovskite NCs as well as carbon-based metal-free QDs have been discovered for both conventional and living radical polymerizations, exhibiting performances similar or superior to those of the metal complexes and organic-based PIs/PCs. Furthermore, benefiting from the unique optical and electronic properties such as high extinction coefficient, giant TPA cross section, etc., SNM-induced photopolymerization methodology offers numerous opportunities in rapid photoinduced 3D printing, harvesting NIR irradiation sources, and fabrication of functional organic−inorganic nanocomposites.

Despite the great achievements in SNM-induced photopolymerization over the past decades, there are still many challenges and unknown potentials in the field. First, most SNMs contain heavy metals that may remain as the contamination in the yielding polymers, which may hinder the biomedical and electronic applications of the resulting polymers.[15] Therefore, the development of metal-free PCs such as carbon nanodots[148] and semiconducting polymer NPs[225] or substitution of high toxicity metal in SNMs with nontoxic metal atoms (Bi, Sb, Zn, etc.) is of general interest.[95,226]

Moreover, expanding the scope of photopolymerization mediated by SNMs is also of particular interest. Currently, SNM-photoinduced polymerizations are limited to radical polymerizations such as RAFT and ATRP via the PET process. Leveraging the cation-rich surface and strong photoinduced hole transfer process of SNMs, we foresee that SNMs could work as PIs/PCs for other types of polymerizations such as cationic polymerizations[19] and ROMP,[20] consequentially extending the monomer accessibility.

Moreover, doping the SNMs with catalytic active metals such as Ni,[112] Au,[227,228] Pd,[229,230] and Ru[231] could favorably influence their charge transfer efficiency, enhance the spatial charge separation, and suppress the radiative charge recombination,[121,123] thus improving the photocatalytic catalytic performance of SNMs.[71,85,232] We believe that heterostructures/nanohybrids forming from conjugating noble metal NPs with semiconductors could also be applied for photopolymerization systems with the rationally designed mechanism.

Furthermore, resolving structure−property−performance relationships[233] would provide a guiding principle for design of efficient SNM PCs. For example, parameters such as energy level,[132] crystal structure,[76] surface ligands,[234] sizes, and shapes of SNMs[177] are determinative to their optoelectronic properties, electron distribution, and catalytic surface area and therefore could highly influence the photocatalytic performance of QDs. Meanwhile, high-throughput techniques[235] and computational calculation[27] should also be robust tools for exploring the PCs' structure−property relationship.

Last but not least, improving the oxygen tolerance[42,236,237] and scalability of SNM-photocatalyzed polymerization would bridge the gap between academic study and industrial applications. For example, building core−shell structures[238]

https://doi.org/10.1021/acspolymersau.1c00014
ACS Polym. Au 2021, 1, 76−99

and adding sacrificial ligands[116] would improve the stability of SNMs and prevent them from photobleaching. In addition, integrating flow systems[239] with SNM-mediated photopolymerizations would provide numerous chances for performing large-scale reactions with an improved polymerization effect.

AUTHOR INFORMATION

Corresponding Author

Eilaf Egap − *Department of Materials Science and Nanoengineering and Department of Chemical and Biomolecular Engineering, Rice University, Houston, Texas 77005, United States;* orcid.org/0000-0002-6106-5276; Email: ee30@rice.edu

Author

Yifan Zhu − *Department of Materials Science and Nanoengineering, Rice University, Houston, Texas 77005, United States;* orcid.org/0000-0002-9816-5764

Complete contact information is available at: https://pubs.acs.org/10.1021/acspolymersau.1c00014

Notes

The authors declare no competing financial interest.

ACKNOWLEDGMENTS

This study is supported by the National Science Foundation (CHE1821863).

REFERENCES

(1) Leibfarth, F. A.; Mattson, K. M.; Fors, B. P.; Collins, H. A.; Hawker, C. J. External Regulation of Controlled Polymerizations. *Angew. Chem., Int. Ed.* **2013**, *52* (1), 199−210.

(2) Chen, M.; Zhong, M.; Johnson, J. A. Light-Controlled Radical Polymerization: Mechanisms, Methods, and Applications. *Chem. Rev.* **2016**, *116* (17), 10167−10211.

(3) Yagci, Y.; Jockusch, S.; Turro, N. J. Photoinitiated Polymerization: Advances, Challenges, and Opportunities. *Macromolecules* **2010**, *43* (15), 6245−6260.

(4) Michaudel, Q.; Kottisch, V.; Fors, B. P. Cationic Polymerization: From Photoinitiation to Photocontrol. *Angew. Chem., Int. Ed.* **2017**, *56* (33), 9670−9679.

(5) Matyjaszewski, K.; Spanswick, J. Controlled/Living Radical Polymerization. *Mater. Today* **2005**, *8* (3), 26−33.

(6) Braunecker, W. A.; Matyjaszewski, K. Controlled/Living Radical Polymerization: Features, Developments, and Perspectives. *Prog. Polym. Sci.* **2007**, *32* (1), 93−146.

(7) Dietlin, C.; Schweizer, S.; Xiao, P.; Zhang, J.; Morlet-Savary, F.; Graff, B.; Fouassier, J. P.; Lalevée, J. Photopolymerization upon LEDs: New Photoinitiating Systems and Strategies. *Polym. Chem.* **2015**, *6* (21), 3895−3912.

(8) Corrigan, N.; Shanmugam, S.; Xu, J.; Boyer, C. Photocatalysis in Organic and Polymer Synthesis. *Chem. Soc. Rev.* **2016**, *45* (22), 6165−6212.

(9) Pan, X.; Tasdelen, M. A.; Laun, J.; Junkers, T.; Yagci, Y.; Matyjaszewski, K. Photomediated Controlled Radical Polymerization. *Prog. Polym. Sci.* **2016**, *62*, 73−125.

(10) Discekici, E. H.; Anastasaki, A.; Read de Alaniz, J.; Hawker, C. J. Evolution and Future Directions of Metal-Free Atom Transfer Radical Polymerization. *Macromolecules* **2018**, *51* (19), 7421−7434.

(11) Theriot, J. C.; McCarthy, B. G.; Lim, C.-H.; Miyake, G. M. Organocatalyzed Atom Transfer Radical Polymerization: Perspectives on Catalyst Design and Performance. *Macromol. Rapid Commun.* **2017**, *38* (13), 1700040.

(12) Dadashi-Silab, S.; Doran, S.; Yagci, Y. Photoinduced Electron Transfer Reactions for Macromolecular Syntheses. *Chem. Rev.* **2016**, *116* (17), 10212−10275.

(13) Chen, D.-F.; Boyle, B. M.; McCarthy, B. G.; Lim, C.-H.; Miyake, G. M. Controlling Polymer Composition in Organocatalyzed Photoredox Radical Ring-Opening Polymerization of Vinylcyclopropanes. *J. Am. Chem. Soc.* **2019**, *141* (33), 13268−13277.

(14) Miyake, G. M.; Theriot, J. C. Perylene as an Organic Photocatalyst for the Radical Polymerization of Functionalized Vinyl Monomers through Oxidative Quenching with Alkyl Bromides and Visible Light. *Macromolecules* **2014**, *47* (23), 8255−8261.

(15) Theriot, J. C.; Lim, C.-H.; Yang, H.; Ryan, M. D.; Musgrave, C. B.; Miyake, G. M. Organocatalyzed Atom Transfer Radical Polymerization Driven by Visible Light. *Science (Washington, DC, U. S.)* **2016**, *352* (6289), 1082−1086.

(16) Pan, X.; Fang, C.; Fantin, M.; Malhotra, N.; So, W. Y.; Peteanu, L. A.; Isse, A. A.; Gennaro, A.; Liu, P.; Matyjaszewski, K. Mechanism of Photoinduced Metal-Free Atom Transfer Radical Polymerization: Experimental and Computational Studies. *J. Am. Chem. Soc.* **2016**, *138* (7), 2411−2425.

(17) Fors, B. P.; Hawker, C. J. Control of a Living Radical Polymerization of Methacrylates by Light. *Angew. Chem., Int. Ed.* **2012**, *51* (35), 8850−8853.

(18) Liu, X.; Zhang, L.; Cheng, Z.; Zhu, X. Metal-Free Photoinduced Electron Transfer-Atom Transfer Radical Polymerization (PET-ATRP) via a Visible Light Organic Photocatalyst. *Polym. Chem.* **2016**, *7* (3), 689−700.

(19) Kottisch, V.; Michaudel, Q.; Fors, B. P. Cationic Polymerization of Vinyl Ethers Controlled by Visible Light. *J. Am. Chem. Soc.* **2016**, *138* (48), 15535−15538.

(20) Ogawa, K. A.; Goetz, A. E.; Boydston, A. J. Metal-Free Ring-Opening Metathesis Polymerization. *J. Am. Chem. Soc.* **2015**, *137* (4), 1400−1403.

(21) Perkowski, A. J.; You, W.; Nicewicz, D. A. Visible Light Photoinitiated Metal-Free Living Cationic Polymerization of 4-Methoxystyrene. *J. Am. Chem. Soc.* **2015**, *137* (24), 7580−7583.

(22) Guillaneuf, Y.; Bertin, D.; Gigmes, D.; Versace, D. L.; Lalevée, J.; Fouassier, J. P. Toward Nitroxide-Mediated Photopolymerization. *Macromolecules* **2010**, *43* (5), 2204−2212.

(23) Chen, D. F.; Bernsten, S.; Miyake, G. M. Organocatalyzed Photoredox Radical Ring-Opening Polymerization of Functionalized Vinylcyclopropanes. *Macromolecules* **2020**, *53* (19), 8352−8359.

(24) Xu, J.; Jung, K.; Atme, A.; Shanmugam, S.; Boyer, C. A Robust and Versatile Photoinduced Living Polymerization of Conjugated and Unconjugated Monomers and Its Oxygen Tolerance. *J. Am. Chem. Soc.* **2014**, *136* (14), 5508−5519.

(25) Xu, J.; Shanmugam, S.; Duong, H. T.; Boyer, C. Organo-Photocatalysts for Photoinduced Electron Transfer-Reversible Addition-Fragmentation Chain Transfer (PET-RAFT) Polymerization. *Polym. Chem.* **2015**, *6* (31), 5615−5624.

(26) Shanmugam, S.; Xu, J.; Boyer, C. Photoinduced Electron Transfer-Reversible Addition-Fragmentation Chain Transfer (PET-RAFT) Polymerization of Vinyl Acetate and *N* -Vinylpyrrolidinone: Kinetic and Oxygen Tolerance Study. *Macromolecules* **2014**, *47* (15), 4930−4942.

(27) Wu, C.; Corrigan, N.; Lim, C. H.; Jung, K.; Zhu, J.; Miyake, G.; Xu, J.; Boyer, C. Guiding the Design of Organic Photocatalyst for PET-RAFT Polymerization: Halogenated Xanthene Dyes. *Macromolecules* **2019**, *52* (1), 236−248.

(28) Figg, C. A.; Hickman, J. D.; Scheutz, G. M.; Shanmugam, S.; Carmean, R. N.; Tucker, B. S.; Boyer, C.; Sumerlin, B. S. Color-Coding Visible Light Polymerizations To Elucidate the Activation of Trithiocarbonates Using Eosin Y. *Macromolecules* **2018**, *51* (4), 1370−1376.

(29) Yeow, J.; Chapman, R.; Xu, J.; Boyer, C. Oxygen Tolerant Photopolymerization for Ultralow Volumes. *Polym. Chem.* **2017**, *8* (34), 5012−5022.

(30) Chen, M.; MacLeod, M. J.; Johnson, J. A. Visible-Light-Controlled Living Radical Polymerization from a Trithiocarbonate

Iniferter Mediated by an Organic Photoredox Catalyst. *ACS Macro Lett.* **2015**, *4* (5), 566−569.
(31) Zhou, Y. N.; Li, J. J.; Wu, Y. Y.; Luo, Z. H. Role of External Field in Polymerization: Mechanism and Kinetics. *Chem. Rev.* **2020**, *120* (5), 2950−3048.
(32) Corrigan, N.; Yeow, J.; Judzewitsch, P.; Xu, J.; Boyer, C. Seeing the Light: Advancing Materials Chemistry through Photopolymerization. *Angew. Chem., Int. Ed.* **2019**, *58* (16), 5170−5189.
(33) Matyjaszewski, K.; Tsarevsky, N. V. Macromolecular Engineering by Atom Transfer Radical Polymerization. *J. Am. Chem. Soc.* **2014**, *136* (18), 6513−6533.
(34) Grubbs, R. B.; Grubbs, R. H. *50th Anniversary Perspective*: Living Polymerization—Emphasizing the *Molecule* in *Macromolecules*. *Macromolecules* **2017**, *50* (18), 6979−6997.
(35) Treat, N. J.; Sprafke, H.; Kramer, J. W.; Clark, P. G.; Barton, B. E.; Read de Alaniz, J.; Fors, B. P.; Hawker, C. J. Metal-Free Atom Transfer Radical Polymerization. *J. Am. Chem. Soc.* **2014**, *136* (45), 16096−16101.
(36) Theriot, J. C.; Miyake, G. M.; Boyer, C. A. *N N* -Diaryl Dihydrophenazines as Photoredox Catalysts for PET-RAFT and Sequential PET-RAFT/O-ATRP. *ACS Macro Lett.* **2018**, *7* (6), 662−666.
(37) Trotta, J.; Fors, B. Organic Catalysts for Photocontrolled Polymerizations. *Synlett* **2016**, *27* (05), 702−713.
(38) Zhang, G.; Song, I. Y.; Ahn, K. H.; Park, T.; Choi, W. Free Radical Polymerization Initiated and Controlled by Visible Light Photocatalysis at Ambient Temperature. *Macromolecules* **2011**, *44* (19), 7594−7599.
(39) Discekici, E. H.; Anastasaki, A.; Kaminker, R.; Willenbacher, J.; Truong, N. P.; Fleischmann, C.; Oschmann, B.; Lunn, D. J.; Read De Alaniz, J.; Davis, T. P.; Bates, C. M.; Hawker, C. J. Light-Mediated Atom Transfer Radical Polymerization of Semi-Fluorinated (Meth)-Acrylates: Facile Access to Functional Materials. *J. Am. Chem. Soc.* **2017**, *139* (16), 5939−5945.
(40) Niu, J.; Page, Z. A.; Dolinski, N. D.; Anastasaki, A.; Hsueh, A. T.; Soh, H. T.; Hawker, C. J. Rapid Visible Light-Mediated Controlled Aqueous Polymerization with In Situ Monitoring. *ACS Macro Lett.* **2017**, *6* (10), 1109−1113.
(41) Xu, J.; Jung, K.; Boyer, C. Oxygen Tolerance Study of Photoinduced Electron Transfer-Reversible Addition-Fragmentation Chain Transfer (PET-RAFT) Polymerization Mediated by Ru(Bpy)-3Cl2. *Macromolecules* **2014**, *47* (13), 4217−4229.
(42) Yeow, J.; Chapman, R.; Gormley, A. J.; Boyer, C. Up in the Air: Oxygen Tolerance in Controlled/Living Radical Polymerisation. *Chem. Soc. Rev.* **2018**, *47* (12), 4357−4387.
(43) Cole, J. P.; Federico, C. R.; Lim, C. H.; Miyake, G. M. Photoinduced Organocatalyzed Atom Transfer Radical Polymerization Using Low Ppm Catalyst Loading. *Macromolecules* **2019**, *52* (2), 747−754.
(44) Ciftci, M.; Yoshikawa, Y.; Yagci, Y. Living Cationic Polymerization of Vinyl Ethers through a Photoinduced Radical Oxidation/Addition/Deactivation Sequence. *Angew. Chem., Int. Ed.* **2017**, *56* (2), 519−523.
(45) Gong, H.; Zhao, Y.; Shen, X.; Lin, J.; Chen, M. Organocatalyzed Photocontrolled Radical Polymerization of Semifluorinated (Meth)Acrylates Driven by Visible Light. *Angew. Chem., Int. Ed.* **2018**, *57* (1), 333−337.
(46) Jiang, K.; Han, S.; Ma, M.; Zhang, L.; Zhao, Y.; Chen, M. Photoorganocatalyzed Reversible-Deactivation Alternating Copolymerization of Chlorotrifluoroethylene and Vinyl Ethers under Ambient Conditions: Facile Access to Main-Chain Fluorinated Copolymers. *J. Am. Chem. Soc.* **2020**, *142* (15), 7108−7115.
(47) Michaudel, Q.; Chauviré, T.; Kottisch, V.; Supej, M. J.; Stawiasz, K. J.; Shen, L.; Zipfel, W. R.; Abruña, H. D.; Freed, J. H.; Fors, B. P. Mechanistic Insight into the Photocontrolled Cationic Polymerization of Vinyl Ethers. *J. Am. Chem. Soc.* **2017**, *139* (43), 15530−15538.
(48) Zhao, Y.; Ma, M.; Lin, X.; Chen, M. Photoorganocatalyzed Divergent Reversible-Deactivation Radical Polymerization towards Linear and Branched Fluoropolymers. *Angew. Chem., Int. Ed.* **2020**, *59* (48), 21470−21474.
(49) Chen, M.; Gu, Y.; Singh, A.; Zhong, M.; Jordan, A. M.; Biswas, S.; Korley, L. T. J.; Balazs, A. C.; Johnson, J. A. Living Additive Manufacturing: Transformation of Parent Gels into Diversely Functionalized Daughter Gels Made Possible by Visible Light Photoredox Catalysis. *ACS Cent. Sci.* **2017**, *3* (2), 124−134.
(50) Wolfbeis, O. S. An Overview of Nanoparticles Commonly Used in Fluorescent Bioimaging. *Chem. Soc. Rev.* **2015**, *44* (14), 4743−4768.
(51) Rogach, A. L.; Gaponik, N.; Lupton, J. M.; Bertoni, C.; Gallardo, D. E.; Dunn, S.; Li Pira, N.; Paderi, M.; Repetto, P.; Romanov, S. G.; O'Dwyer, C.; Sotomayor Torres, C. M.; Eychmüller, A. Light-Emitting Diodes with Semiconductor Nanocrystals. *Angew. Chem., Int. Ed.* **2008**, *47* (35), 6538−6549.
(52) Kamat, P. V. Quantum Dot Solar Cells. Semiconductor Nanocrystals as Light Harvesters. *J. Phys. Chem. C* **2008**, *112* (48), 18737−18753.
(53) Smith, A. M.; Nie, S. Semiconductor Nanocrystals: Structure, Properties, and Band Gap Engineering. *Acc. Chem. Res.* **2010**, *43* (2), 190−200.
(54) Zhu, Y.; Liu, Y.; Miller, K. A.; Zhu, H.; Egap, E. Lead Halide Perovskite Nanocrystals as Photocatalysts for PET-RAFT Polymerization under Visible and Near-Infrared Irradiation. *ACS Macro Lett.* **2020**, *9* (5), 725−730.
(55) Alivisatos, A. P. Semiconductor Clusters, Nanocrystals, and Quantum Dots. *Science (Washington, DC, U. S.)* **1996**, *271* (5251), 933−937.
(56) Yu, W. W.; Peng, X. Formation of High-Quality CdS and Other II-VI Semiconductor Nanocrystals in Noncoordinating Solvents: Tunable Reactivity of Monomers. *Angew. Chem., Int. Ed.* **2002**, *41* (13), 2368−2371.
(57) Huang, H.; Pradhan, B.; Hofkens, J.; Roeffaers, M. B. J.; Steele, J. A. Solar-Driven Metal Halide Perovskite Photocatalysis: Design, Stability, and Performance. *ACS Energy Lett.* **2020**, *5* (4), 1107−1123.
(58) Li, X. B.; Tung, C. H.; Wu, L. Z. Semiconducting Quantum Dots for Artificial Photosynthesis. *Nat. Rev. Chem.* **2018**, *2* (8), 160−173.
(59) Han, C.; Zhu, X.; Martin, J. S.; Lin, Y.; Spears, S.; Yan, Y. Recent Progress in Engineering Metal Halide Perovskites for Efficient Visible-Light-Driven Photocatalysis. *ChemSusChem* **2020**, *13* (16), 4005−4025.
(60) Kodaimati, M. S.; McClelland, K. P.; He, C.; Lian, S.; Jiang, Y.; Zhang, Z.; Weiss, E. A. Viewpoint: Challenges in Colloidal Photocatalysis and Some Strategies for Addressing Them. *Inorg. Chem.* **2018**, *57* (7), 3659−3670.
(61) Liu, M.; Peng, T.; Li, H.; Zhao, L.; Sang, Y.; Feng, Q.; Xu, L.; Jiang, Y.; Liu, H.; Zhang, J. Photoresponsive Nanostructure Assisted Green Synthesis of Organics and Polymers. *Appl. Catal., B* **2019**, *249*, 172−210.
(62) Pan, X.; Fantin, M.; Yuan, F.; Matyjaszewski, K. Externally Controlled Atom Transfer Radical Polymerization. *Chem. Soc. Rev.* **2018**, *47* (14), 5457−5490.
(63) Shao, J.; Huang, Y.; Fan, Q. Visible Light Initiating Systems for Photopolymerization: Status, Development and Challenges. *Polym. Chem.* **2014**, *5* (14), 4195−4210.
(64) Doerr, A. M.; Burroughs, J. M.; Gitter, S. R.; Yang, X.; Boydston, A. J.; Long, B. K. Advances in Polymerizations Modulated by External Stimuli. *ACS Catal.* **2020**, *10* (24), 14457−14515.
(65) An, Z.; Zhu, S.; An, Z. Heterogeneous Photocatalytic Reversible Deactivation Radical Polymerization. *Polym. Chem.* **2021**, *12* (16), 2357−2373.
(66) Waiskopf, N.; Magdassi, S.; Banin, U. Quantum Photoinitiators: Toward Emerging Photocuring Applications. *J. Am. Chem. Soc.* **2021**, *143* (2), 577−587.
(67) Cumpston, B. H.; Ananthavel, S. P.; Barlow, S.; Dyer, D. L.; Ehrlich, J. E.; Erskine, L. L.; Heikal, A. A.; Kuebler, S. M.; Lee, I.-Y. Y. S.; McCord-Maughon, D.; Qin, J.; Röckel, H.; Rumi, M.; Wu, X. L.; Marder, S. R.; Perry, J. W. Two-Photon Polymerization Initiators for

Three-Dimensional Optical Data Storage and Microfabrication. *Nature* **1999**, *398* (6722), 51−54.
(68) Hoffman, A. J.; Yee, H.; Mills, G.; Hoffmann, M. R. Photoinitiated Polymerization of Methyl Methacrylate Using Q-Sized Zinc Oxide Colloids. *J. Phys. Chem.* **1992**, *96* (13), 5540−5546.
(69) Popović, I. G.; Katsikas, L.; Müller, U.; Veličković, J. S.; Weller, H. The Homogeneous Photopolymerization of Methyl Methacrylate by Colloidal Cadmium Sulfide. *Macromol. Chem. Phys.* **1994**, *195* (3), 889−904.
(70) Strandwitz, N. C.; Khan, A.; Boettcher, S. W.; Mikhailovsky, A. A.; Hawker, C. J.; Nguyen, T.-Q.; Stucky, G. D. One-and Two-Photon Induced Polymerization of Methylmethacrylate Using Colloidal CdS Semiconductor Quantum Dots. *J. Am. Chem. Soc.* **2008**, *130* (26), 8280−8288.
(71) Verbitsky, L.; Waiskopf, N.; Magdassi, S.; Banin, U. A Clear Solution: Semiconductor Nanocrystals as Photoinitiators in Solvent Free Polymerization. *Nanoscale* **2019**, *11* (23), 11209−11216.
(72) Anyaogu, K. C.; Cai, X.; Neckers, D. C. Gold Nanoparticle Photopolymerization of Acrylates. *Macromolecules* **2008**, *41* (23), 9000−9003.
(73) Ding, T.; Mertens, J.; Lombardi, A.; Scherman, O. A.; Baumberg, J. J. Light-Directed Tuning of Plasmon Resonances via Plasmon-Induced Polymerization Using Hot Electrons. *ACS Photonics* **2017**, *4* (6), 1453−1458.
(74) Wang, C.; Astruc, D. Nanogold Plasmonic Photocatalysis for Organic Synthesis and Clean Energy Conversion. *Chem. Soc. Rev.* **2014**, *43* (20), 7188−7216.
(75) Wang, Y.; Wang, S.; Zhang, S.; Scherman, O. A.; Baumberg, J. J.; Ding, T.; Xu, H. Plasmon-Directed Polymerization: Regulating Polymer Growth with Light. *Nano Res.* **2018**, *11* (12), 6384−6390.
(76) Jiang, J.; Ye, G.; Lorandi, F.; Liu, Z.; Liu, Y.; Hu, T.; Chen, J.; Lu, Y.; Matyjaszewski, K. Localized Surface Plasmon Resonance Meets Controlled/Living Radical Polymerization: An Adaptable Strategy for Broadband Light-Regulated Macromolecular Synthesis. *Angew. Chem., Int. Ed.* **2019**, *58* (35), 12096−12101.
(77) Kiskan, B.; Zhang, J.; Wang, X.; Antonietti, M.; Yagci, Y. Mesoporous Graphitic Carbon Nitride as a Heterogeneous Visible Light Photoinitiator for Radical Polymerization. *ACS Macro Lett.* **2012**, *1* (5), 546−549.
(78) Anyaogu, K. C.; Cai, X.; Neckers, D. C. Gold Nanoparticle Photosensitized Radical Photopolymerization. *Photochem. Photobiol. Sci.* **2008**, *7* (12), 1469.
(79) Dadashi-Silab, S.; Asiri, A. M.; Khan, S. B.; Alamry, K. A.; Yagci, Y. Semiconductor Nanoparticles for Photoinitiation of Free Radical Polymerization in Aqueous and Organic Media. *J. Polym. Sci., Part A: Polym. Chem.* **2014**, *52* (10), 1500−1507.
(80) Nakashima, T.; Sakashita, M.; Nonoguchi, Y.; Kawai, T. Sensitized Photopolymerization of an Ionic Liquid-Based Monomer by Using CdTe Nanocrystals. *Macromolecules* **2007**, *40* (18), 6540−6544.
(81) Dule, M.; Biswas, M.; Biswas, Y.; Mandal, T. K. Redox-Active Poly(Ionic Liquid)-Engineered Ag Nanoparticle-Decorated ZnO Nanoflower Heterostructure: A Reusable Composite Catalyst for Photopolymerization into High-Molecular-Weight Polymers. *Polymer* **2017**, *133*, 223−231.
(82) Stroyuk, A. L.; Granchak, V. M.; Korzhak, A. V.; Kuchmii, S. Y. Photoinitiation of Buthylmethacrylate Polymerization by Colloidal Semiconductor Nanoparticles. *J. Photochem. Photobiol., A* **2004**, *162* (2−3), 339−351.
(83) Stroyuk, A. L.; Granchak, V. M.; Kuchmii, S. Y. Photopolymerization of Butyl Methacrylate Initiated by Hydrated Ferric Oxide Nanoparticles. *Theor. Exp. Chem.* **2001**, *37* (6), 350−354.
(84) Zhang, J.; Huang, Y.; Jin, X.; Nazartchouk, A.; Liu, M.; Tong, X.; Jiang, Y.; Ni, L.; Sun, S.; Sang, Y.; Liu, H.; Razzari, L.; Vetrone, F.; Claverie, J. Plasmon Enhanced Upconverting Core@triple-Shell Nanoparticles as Recyclable Panchromatic Initiators (Blue to Infrared) for Radical Polymerization. *Nanoscale Horizons* **2019**, *4* (4), 907−917.
(85) Pawar, A. A.; Halivni, S.; Waiskopf, N.; Ben-Shahar, Y.; Soreni-Harari, M.; Bergbreiter, S.; Banin, U.; Magdassi, S. Rapid Three-Dimensional Printing in Water Using Semiconductor-Metal Hybrid Nanoparticles as Photoinitiators. *Nano Lett.* **2017**, *17* (7), 4497−4501.
(86) Ni, X.; Ye, J.; Dong, C. Kinetics Studies of Methyl Methacrylate Photopolymerization Initiated by Titanium Dioxide Semiconductor Nanoparticles. *J. Photochem. Photobiol., A* **2006**, *181* (1), 19−27.
(87) Tan, J.; Dai, X.; Zhang, Y.; Yu, L.; Sun, H.; Zhang, L. Photoinitiated Polymerization-Induced Self-Assembly via Visible Light-Induced RAFT-Mediated Emulsion Polymerization. *ACS Macro Lett.* **2019**, *8* (2), 205−212.
(88) Dadashi-Silab, S.; Atilla Tasdelen, M.; Mohamed Asiri, A.; Bahadar Khan, S.; Yagci, Y. Photoinduced Atom Transfer Radical Polymerization Using Semiconductor Nanoparticles. *Macromol. Rapid Commun.* **2014**, *35* (4), 454−459.
(89) Tsarevsky, N. V.; Matyjaszewski, K. Green" Atom Transfer Radical Polymerization: From Process Design to Preparation of Well-Defined Environmentally Friendly Polymeric Materials. *Chem. Rev.* **2007**, *107* (6), 2270−2299.
(90) McKenzie, T. G.; Fu, Q.; Uchiyama, M.; Satoh, K.; Xu, J.; Boyer, C.; Kamigaito, M.; Qiao, G. G. Beyond Traditional RAFT: Alternative Activation of Thiocarbonylthio Compounds for Controlled Polymerization. *Adv. Sci.* **2016**, *3* (9), 1500394.
(91) Dadashi-Silab, S.; Lorandi, F.; DiTucci, M. J.; Sun, M.; Szczepaniak, G.; Liu, T.; Matyjaszewski, K. Conjugated Cross-Linked Phenothiazines as Green or Red Light Heterogeneous Photocatalysts for Copper-Catalyzed Atom Transfer Radical Polymerization. *J. Am. Chem. Soc.* **2021**, *143* (25), 9630−9638.
(92) Dolinski, N. D.; Page, Z. A.; Discekici, E. H.; Meis, D.; Lee, I.; Jones, G. R.; Whitfield, R.; Pan, X.; McCarthy, B. G.; Shanmugam, S.; et al. What Happens in the Dark? Assessing the Temporal Control of Photo-mediated Controlled Radical Polymerizations. *J. Polym. Sci., Part A: Polym. Chem.* **2019**, *57* (3), 268−273.
(93) Huang, Y.; Zhu, Y.; Egap, E. Semiconductor Quantum Dots as Photocatalysts for Controlled Light-Mediated Radical Polymerization. *ACS Macro Lett.* **2018**, *7* (2), 184−189.
(94) Djurišić, A. B.; Leung, Y. H.; Ching Ng, A. M. Strategies for Improving the Efficiency of Semiconductor Metal Oxide Photocatalysis. *Mater. Horiz.* **2014**, *1* (4), 400−410.
(95) Hakobyan, K.; Gegenhuber, T.; McErlean, C. S. P.; Müllner, M. Visible-Light-Driven MADIX Polymerisation via a Reusable, Low-Cost, and Non-Toxic Bismuth Oxide Photocatalyst. *Angew. Chem., Int. Ed.* **2019**, *58* (6), 1828−1832.
(96) Adhikari, S. P.; Dean, H.; Hood, Z. D.; Peng, R.; More, K. L.; Ivanov, I.; Wu, Z.; Lachgar, A. Visible-Light-Driven Bi2O3/WO3 Composites with Enhanced Photocatalytic Activity. *RSC Adv.* **2015**, *5* (111), 91094−91102.
(97) Chung, H. Y.; Chen, W.; Wen, X.; Hart, J. N.; Wu, H.; Lai, Y.; Amal, R.; Ng, Y. H. Oxygen-Deficient Bismuth Tungstate and Bismuth Oxide Composite Photoanode with Improved Photostability. *Sci. Bull.* **2018**, *63* (15), 990−996.
(98) Zhang, J.; Zhang, X.; Zhang, J. Y. Size-Dependent Time-Resolved Photoluminescence of Colloidal Cdse Nanocrystals. *J. Phys. Chem. C* **2009**, *113* (22), 9512−9515.
(99) Zhang, Z.; Edme, K.; Lian, S.; Weiss, E. A. Enhancing the Rate of Quantum-Dot-Photocatalyzed Carbon-Carbon Coupling by Tuning the Composition of the Dot's Ligand Shell. *J. Am. Chem. Soc.* **2017**, *139* (12), 4246−4249.
(100) Reiss, P.; Protière, M.; Li, L. Core/Shell Semiconductor Nanocrystals. *Small* **2009**, *5* (2), 154−168.
(101) Ravi, V. K.; Markad, G. B.; Nag, A. Band Edge Energies and Excitonic Transition Probabilities of Colloidal CsPbX3 (X = Cl, Br, I) Perovskite Nanocrystals. *ACS Energy Lett.* **2016**, *1* (4), 665−671.
(102) Zhu, X.; Lin, Y.; Sun, Y.; Beard, M. C.; Yan, Y. Lead-Halide Perovskites for Photocatalytic α-Alkylation of Aldehydes. *J. Am. Chem. Soc.* **2019**, *141* (2), 733−738.
(103) Jiang, J.; Ye, G.; Wang, Z.; Lu, Y.; Chen, J.; Matyjaszewski, K. Heteroatom-Doped Carbon Dots (CDs) as a Class of Metal-Free

Photocatalysts for PET-RAFT Polymerization under Visible Light and Sunlight. *Angew. Chem., Int. Ed.* **2018**, *57* (37), 12037−12042.
(104) Xu, Q.; Kuang, T.; Liu, Y.; Cai, L.; Peng, X.; Sreenivasan Sreeprasad, T.; Zhao, P.; Yu, Z.; Li, N. Heteroatom-Doped Carbon Dots: Synthesis, Characterization, Properties, Photoluminescence Mechanism and Biological Applications. *J. Mater. Chem. B* **2016**, *4* (45), 7204−7219.
(105) Wang, R.; Lu, K. Q.; Tang, Z. R.; Xu, Y. J. Recent Progress in Carbon Quantum Dots: Synthesis, Properties and Applications in Photocatalysis. *J. Mater. Chem. A* **2017**, *5* (8), 3717−3734.
(106) Tokumoto, M. S.; Briois, V.; Santilli, C. V.; Pulcinelli, S. H. Preparation of ZnO Nanoparticles: Structural Study of the Molecular Precursor. *J. Sol-Gel Sci. Technol.* **2003**, *26* (1−3), 547−551.
(107) Zhang, Z. Y.; Xiong, H. M. Photoluminescent ZnO Nanoparticles and Their Biological Applications. *Materials* **2015**, *8* (6), 3101−3127.
(108) Damm, C.; Herrmann, R.; Israel, G.; Müller, F. W. Acrylate Photopolymerization on Heterostructured TiO2 Photocatalysts. *Dyes Pigm.* **2007**, *74* (2), 335−342.
(109) Siriwong, C.; Wetchakun, N.; Inceesungvorn, B.; Channei, D.; Samerjai, T.; Phanichphant, S. Doped-Metal Oxide Nanoparticles for Use as Photocatalysts. *Prog. Cryst. Growth Charact. Mater.* **2012**, *58* (2−3), 145−163.
(110) Hakobyan, K.; McErlean, C. S. P.; Müllner, M. Activating ATRP Initiators to Incorporate End-Group Modularity into Photo-RAFT Polymerization. *Macromolecules* **2020**, *53* (23), 10357−10365.
(111) Caputo, J. A.; Frenette, L. C.; Zhao, N.; Sowers, K. L.; Krauss, T. D.; Weix, D. J. General and Efficient C-C Bond Forming Photoredox Catalysis with Semiconductor Quantum Dots. *J. Am. Chem. Soc.* **2017**, *139* (12), 4250−4253.
(112) Li, X.-B.; Li, Z.-J.; Gao, Y.-J.; Meng, Q.-Y.; Yu, S.; Weiss, R. G.; Tung, C.-H.; Wu, L.-Z. Mechanistic Insights into the Interface-Directed Transformation of Thiols into Disulfides and Molecular Hydrogen by Visible-Light Irradiation of Quantum Dots. *Angew. Chem., Int. Ed.* **2014**, *53* (8), 2085−2089.
(113) Zhao, L. M.; Meng, Q. Y.; Fan, X. B.; Ye, C.; Li, X. B.; Chen, B.; Ramamurthy, V.; Tung, C. H.; Wu, L. Z. Photocatalysis with Quantum Dots and Visible Light: Selective and Efficient Oxidation of Alcohols to Carbonyl Compounds through a Radical Relay Process in Water. *Angew. Chem., Int. Ed.* **2017**, *56* (11), 3020−3024.
(114) Xi, Z. W.; Yang, L.; Wang, D. Y.; Pu, C. D.; Shen, Y. M.; Wu, C. De; Peng, X. G. Visible-Light Photocatalytic Synthesis of Amines from Imines via Transfer Hydrogenation Using Quantum Dots as Catalysts. *J. Org. Chem.* **2018**, *83* (19), 11886−11895.
(115) Zhu, Y.; Jin, T.; Lian, T.; Egap, E. Enhancing the Efficiency of Semiconducting Quantum Dot Photocatalyzed Atom Transfer Radical Polymerization by Ligand Shell Engineering. *J. Chem. Phys.* **2021**, *154* (20), 204903.
(116) Weiss, E. A. Designing the Surfaces of Semiconductor Quantum Dots for Colloidal Photocatalysis. *ACS Energy Lett.* **2017**, *2* (5), 1005−1013.
(117) Yu, W. W.; Qu, L.; Guo, W.; Peng, X. Experimental Determination of the Extinction Coefficient of CdTe, CdSe, and CdS Nanocrystals. *Chem. Mater.* **2003**, *15* (14), 2854−2860.
(118) Jasieniak, J.; Califano, M.; Watkins, S. E. Size-Dependent Valence and Conduction Band-Edge Energies of Semiconductor Nanocrystals. *ACS Nano* **2011**, *5* (7), 5888−5902.
(119) Jin, T.; Uhlikova, N.; Xu, Z.; Zhu, Y.; Huang, Y.; Egap, E.; Lian, T. Enhanced Triplet State Generation through Radical Pair Intermediates in BODIPY-Quantum Dot Complexes. *J. Chem. Phys.* **2019**, *151* (24), 241101.
(120) Jin, T.; Uhlikova, N.; Xu, Z.; Zhu, Y.; Huang, Y.; Egap, E.; Lian, T. Competition of Dexter, Förster, and Charge Transfer Pathways for Quantum Dot Sensitized Triplet Generation. *J. Chem. Phys.* **2020**, *152* (21), 214702.
(121) Banin, U.; Ben-Shahar, Y.; Vinokurov, K. Hybrid Semiconductor-Metal Nanoparticles: From Architecture to Function. *Chem. Mater.* **2014**, *26* (1), 97−110.
(122) Jia, G.; Pang, Y.; Ning, J.; Banin, U.; Ji, B. Heavy-Metal-Free Colloidal Semiconductor Nanorods: Recent Advances and Future Perspectives. *Adv. Mater.* **2019**, *31*, 1900781.
(123) Waiskopf, N.; Ben-Shahar, Y.; Banin, U. Photocatalytic Hybrid Semiconductor-Metal Nanoparticles; from Synergistic Properties to Emerging Applications. *Adv. Mater.* **2018**, *30* (41), 1706697.
(124) Waiskopf, N.; Ben-Shahar, Y.; Galchenko, M.; Carmel, I.; Moshitzky, G.; Soreq, H.; Banin, U. Photocatalytic Reactive Oxygen Species Formation by Semiconductor-Metal Hybrid Nanoparticles. Toward Light-Induced Modulation of Biological Processes. *Nano Lett.* **2016**, *16* (7), 4266−4273.
(125) Zhao, Y.; Zhu, K. Organic-Inorganic Hybrid Lead Halide Perovskites for Optoelectronic and Electronic Applications. *Chem. Soc. Rev.* **2016**, *45* (3), 655−689.
(126) Cho, H.; Jeong, S.-H.; Park, M.-H.; Kim, Y.-H.; Wolf, C.; Lee, C.-L.; Heo, J. H.; Sadhanala, A.; Myoung, N.; Yoo, S.; Im, S. H.; Friend, R. H.; Lee, T.-W. Overcoming the Electroluminescence Efficiency Limitations of Perovskite Light-Emitting Diodes. *Science (Washington, DC, U. S.)* **2015**, *350* (6265), 1222−1225.
(127) Huang, H.; Bodnarchuk, M. I.; Kershaw, S. V.; Kovalenko, M. V.; Rogach, A. L. Lead Halide Perovskite Nanocrystals in the Research Spotlight: Stability and Defect Tolerance. *ACS Energy Lett.* **2017**, *2* (9), 2071−2083.
(128) Wang, Y.; Wu, J.; Zhang, P.; Liu, D.; Zhang, T.; Ji, L.; Gu, X.; David Chen, Z.; Li, S. Stitching Triple Cation Perovskite by a Mixed Anti-Solvent Process for High Performance Perovskite Solar Cells. *Nano Energy* **2017**, *39*, 616−625.
(129) Protesescu, L.; Yakunin, S.; Bodnarchuk, M. I.; Krieg, F.; Caputo, R.; Hendon, C. H.; Yang, R. X.; Walsh, A.; Kovalenko, M. V. Nanocrystals of Cesium Lead Halide Perovskites (CsPbX3, X = Cl, Br, and I): Novel Optoelectronic Materials Showing Bright Emission with Wide Color Gamut. *Nano Lett.* **2015**, *15* (6), 3692−3696.
(130) Saparov, B.; Mitzi, D. B. Organic-Inorganic Perovskites: Structural Versatility for Functional Materials Design. *Chem. Rev.* **2016**, *116* (7), 4558−4596.
(131) Mei, A.; Li, X.; Liu, L.; Ku, Z.; Liu, T.; Rong, Y.; Xu, M.; Hu, M.; Chen, J.; Yang, Y.; Grätzel, M.; Han, H. A Hole-Conductor-Free, Fully Printable Mesoscopic Perovskite Solar Cell with High Stability. *Science (Washington, DC, U. S.)* **2014**, *345* (6194), 295−298.
(132) Zhu, X.; Lin, Y.; San Martin, J.; Sun, Y.; Zhu, D.; Yan, Y. Lead Halide Perovskites for Photocatalytic Organic Synthesis. *Nat. Commun.* **2019**, *10* (1), 2843.
(133) Hong, Z.; Chong, W. K.; Ng, A. Y. R.; Li, M.; Ganguly, R.; Sum, T. C.; Soo, H. S. Hydrophobic Metal Halide Perovskites for Visible-Light Photoredox C-C Bond Cleavage and Dehydrogenation Catalysis. *Angew. Chem., Int. Ed.* **2019**, *58* (11), 3456−3460.
(134) Nicewicz, D. A.; MacMillan, D. W. C. Merging Photoredox Catalysis with Organocatalysis: The Direct Asymmetric Alkylation of Aldehydes. *Science* **2008**, *322* (5898), 77−80.
(135) Chen, K.; Deng, X.; Dodekatos, G.; Tüysüz, H. Photocatalytic Polymerization of 3,4-Ethylenedioxythiophene over Cesium Lead Iodide Perovskite Quantum Dots. *J. Am. Chem. Soc.* **2017**, *139* (35), 12267−12273.
(136) Wong, Y.-C.; De Andrew Ng, J.; Tan, Z.-K. Perovskite-Initiated Photopolymerization for Singly Dispersed Luminescent Nanocomposites. *Adv. Mater.* **2018**, *30* (21), 1800774.
(137) Li, Y.; Shu, Q.; Du, Q.; Dai, Y.; Zhao, S.; Zhang, J.; Li, L.; Chen, K. Surface Modification for Improving the Photocatalytic Polymerization of 3,4-Ethylenedioxythiophene over Inorganic Lead Halide Perovskite Quantum Dots. *ACS Appl. Mater. Interfaces* **2020**, *12* (1), 451−460.
(138) Lv, W.; Li, L.; Xu, M.; Hong, J.; Tang, X.; Xu, L.; Wu, Y.; Zhu, R.; Chen, R.; Huang, W. Improving the Stability of Metal Halide Perovskite Quantum Dots by Encapsulation. *Adv. Mater.* **2019**, *31* (28), 1900682.
(139) Mollick, S.; Mandal, T. N.; Jana, A.; Fajal, S.; Desai, A. V.; Ghosh, S. K. Ultrastable Luminescent Hybrid Bromide Perovskite@MOF Nanocomposites for the Degradation of Organic Pollutants in Water. *ACS Appl. Nano Mater.* **2019**, *2* (3), 1333−1340.

(140) Liu, Y.; Zhu, Y.; Alahakoon, S. B.; Egap, E. Synthesis of Imine-Based Covalent Organic Frameworks Catalyzed by Metal Halides and in Situ Growth of Perovskite@COF Composites. *ACS Mater. Lett.* **2020**, *2*, 1561−1566.
(141) Liu, X.; Dai, L. Carbon-Based Metal-Free Catalysts. *Nat. Rev. Mater.* **2016**, *1* (11), 16064.
(142) Wu, X.; Chen, D.-F.; Chen, S.-S.; Zhu, Y.-F. Synthesis of Polycyclic Amines through Mild Metal-Free Tandem Cross-Dehydrogenative Coupling/Intramolecular Hydroarylation of N-Aryltetrahydroisoquinolines and Crotonaldehyde. *Eur. J. Org. Chem.* **2015**, *2015* (3), 468−473.
(143) Huang, J.-Z.; Zhang, C.-L.; Zhu, Y.-F.; Li, L.-L.; Chen, D.-F.; Han, Z.-Y.; Gong, L.-Z. Organocatalytic Highly Enantioselective Substitution of 3-(1-Tosylalkyl)Indoles with Oxindoles Enables the First Total Synthesis of (+)-Trigolutes B. *Chem. - Eur. J.* **2015**, *21* (23), 8389−8393.
(144) Kütahya, C.; Wang, P.; Li, S.; Liu, S.; Li, J.; Chen, Z.; Strehmel, B. Carbon Dots as a Promising Green Photocatalyst for Free Radical and ATRP-Based Radical Photopolymerization with Blue LEDs. *Angew. Chem., Int. Ed.* **2020**, *59* (8), 3166−3171.
(145) Lu, M. Photoinduced Atom Transfer Radical Polymerization of Methyl Methacrylate with Conducting Polymer Nanostructures as Photocatalyst. *Iran. Polym. J.* **2019**, *28* (2), 167−172.
(146) Xia, L.; Cheng, B. F.; Zeng, T. Y.; Nie, X.; Chen, G.; Zhang, Z.; Zhang, W. J.; Hong, C. Y.; You, Y. Z. Polymer Nanofibers Exhibiting Remarkable Activity in Driving the Living Polymerization under Visible Light and Reusability. *Adv. Sci.* **2020**, *7* (6), 1902451.
(147) Fu, Q.; Ruan, Q.; McKenzie, T. G.; Reyhani, A.; Tang, J.; Qiao, G. G. Development of a Robust PET-RAFT Polymerization Using Graphitic Carbon Nitride ($g\text{-}C_3N_4$). *Macromolecules* **2017**, *50* (19), 7509−7516.
(148) Hutton, G. A. M.; Martindale, B. C. M.; Reisner, E. Carbon Dots as Photosensitisers for Solar-Driven Catalysis. *Chem. Soc. Rev.* **2017**, *46* (20), 6111−6123.
(149) Ryan, M. D.; Pearson, R. M.; French, T. A.; Miyake, G. M. Impact of Light Intensity on Control in Photoinduced Organocatalyzed Atom Transfer Radical Polymerization. *Macromolecules* **2017**, *50* (12), 4616−4622.
(150) Yamamoto, M.; Oster, G. Zinc Oxide-Sensitized Photopolymerization. *J. Polym. Sci., Part A-1: Polym. Chem.* **1966**, *4* (7), 1683−1688.
(151) Kuriacose, J. C.; Markham, M. C. Mechanism of the Photo-Initiated Polymerization of Methyl Methacrylate at Zinc Oxide Surfaces 1. *J. Phys. Chem.* **1961**, *65* (12), 2232−2236.
(152) Kamat, P. V.; Basheer, R.; Fox, M. A. Polymer-Modified Electrodes. Electrochemical and Photoelectrochemical Polymerization of 1-Vinylpyrene. *Macromolecules* **1985**, *18* (7), 1366−1371.
(153) Hoffman, A. J.; Mills, G.; Yee, H.; Hoffmann, M. R. Q-Sized Cadmium Sulfide: Synthesis, Characterization, and Efficiency of Photoinitiation of Polymerization of Several Vinylic Monomers. *J. Phys. Chem.* **1992**, *96* (13), 5546−5552.
(154) Huang, Z. Y.; Barber, T.; Mills, G.; Morris, M. B. Heterogeneous Photopolymerization of Methyl Methacrylate Initiated by Small ZnO Particles. *J. Phys. Chem.* **1994**, *98* (48), 12746−12752.
(155) Ojah, R.; Dolui, S. K. Photopolymerization of Methyl Methacrylate Using Dye-Sensitized Semiconductor Based Photocatalyst. *J. Photochem. Photobiol., A* **2005**, *172* (2), 121−125.
(156) Katsikas, L.; Veličković, J. S.; Weller, H.; Popović, I. G. Thermogravimetric Characterisation of Poly(Methyl Methacrylate) Photopolymerised by Colloidal Cadmium Sulphide. *J. Therm. Anal.* **1997**, *49* (1), 317−323.
(157) Dong, C.; Ni, X. The Photopolymerization and Characterization of Methyl Methacrylate Initiated by Nanosized Titanium Dioxide. *J. Macromol. Sci., Part A: Pure Appl.Chem.* **2004**, *41* (5), 547−563.
(158) Furst, L.; Matsuura, B. S.; Narayanam, J. M. R.; Tucker, J. W.; Stephenson, C. R. J. Visible Light-Mediated Intermolecular C-H Functionalization of Electron-Rich Heterocycles with Malonates. *Org. Lett.* **2010**, *12* (13), 3104−3107.
(159) Alivisatos, A. P. Perspectives on the Physical Chemistry of Semiconductor Nanocrystals. *J. Phys. Chem.* **1996**, *100* (31), 13226−13239.
(160) Dadashi-Silab, S.; Yar, Y.; Yagci Acar, H.; Yagci, Y. Magnetic Iron Oxide Nanoparticles as Long Wavelength Photoinitiators for Free Radical Polymerization. *Polym. Chem.* **2015**, *6* (11), 1918−1922.
(161) Schmitt, M. Synthesis and Testing of ZnO Nanoparticles for Photo-Initiation: Experimental Observation of Two Different Non-Migration Initiators for Bulk Polymerization. *Nanoscale* **2015**, *7* (21), 9532−9544.
(162) Schmitt, M. ZnO Nanoparticle Induced Photo-Kolbe Reaction, Fragment Stabilization and Effect on Photopolymerization Monitored by Raman-UV-Vis Measurements. *Macromol. Chem. Phys.* **2012**, *213* (18), 1953−1962.
(163) Schmitt, M.; Becker, D.; Lalevée, J. Performance Analysis of the Solidification of Acrylic Esters Photo-Initiated by Systematically Modified ZnO Nanoparticles. *Polymer* **2018**, *158*, 83−89.
(164) Liao, W.; Ni, X. Photocatalytic Decarboxylation of Diacids for the Initiation of Free Radical Polymerization. *Photochem. Photobiol. Sci.* **2017**, *16* (8), 1211−1219.
(165) Weng, Z.; Ni, X.; Yang, D.; Wang, J.; Chen, W. Novel Photopolymerizations Initiated by Alkyl Radicals Generated from Photocatalyzed Decarboxylation of Carboxylic Acids over Oxide Semiconductor Nanoparticles: Extended Photo-Kolbe Reactions. *J. Photochem. Photobiol., A* **2009**, *201* (2−3), 151−156.
(166) Dadashi-Silab, S.; Tasdelen, M. A.; Kiskan, B.; Wang, X.; Antonietti, M.; Yagci, Y. Photochemically Mediated Atom Transfer Radical Polymerization Using Polymeric Semiconductor Mesoporous Graphitic Carbon Nitride. *Macromol. Chem. Phys.* **2014**, *215* (7), 675−681.
(167) Yan, J.; Li, B.; Zhou, F.; Liu, W. Ultraviolet Light-Induced Surface-Initiated Atom-Transfer Radical Polymerization. *ACS Macro Lett.* **2013**, *2* (7), 592−596.
(168) Bansal, A.; Kumar, A.; Kumar, P.; Bojja, S.; Chatterjee, A. K.; Ray, S. S.; Jain, S. L. Visible Light-Induced Surface Initiated Atom Transfer Radical Polymerization of Methyl Methacrylate on Titania/Reduced Graphene Oxide Nanocomposite. *RSC Adv.* **2015**, *5* (27), 21189−21196.
(169) Cao, H.; Wang, G.; Xue, Y.; Yang, G.; Tian, J.; Liu, F.; Zhang, W. Far-Red Light-Induced Reversible Addition-Fragmentation Chain Transfer Polymerization Using a Man-Made Bacteriochlorin. *ACS Macro Lett.* **2019**, 616−622.
(170) Cao, Y.; Xu, Y.; Zhang, J.; Yang, D.; Liu, J. Well-Controlled Atom Transfer Radical Polymerizations of Acrylates Using Recyclable Niobium Complex Nanoparticle as Photocatalyst under Visible Light Irradiation. *Polymer* **2015**, *61*, 198−203.
(171) Lim, C. H.; Ryan, M. D.; McCarthy, B. G.; Theriot, J. C.; Sartor, S. M.; Damrauer, N. H.; Musgrave, C. B.; Miyake, G. M. Intramolecular Charge Transfer and Ion Pairing in N, N-Diaryl Dihydrophenazine Photoredox Catalysts for Efficient Organocatalyzed Atom Transfer Radical Polymerization. *J. Am. Chem. Soc.* **2017**, *139* (1), 348−355.
(172) Keddie, D. J.; Moad, G.; Rizzardo, E.; Thang, S. H. RAFT Agent Design and Synthesis. *Macromolecules* **2012**, *45* (13), 5321−5342.
(173) Zhang, J.; Li, A.; Liu, H.; Yang, D.; Liu, J. Well-Controlled RAFT Polymerization Initiated by Recyclable Surface-Modified Nb(OH)5 Nanoparticles under Visible Light Irradiation. *J. Polym. Sci., Part A: Polym. Chem.* **2014**, *52* (19), 2715−2724.
(174) Liu, G.; Shi, H.; Cui, Y.; Tong, J.; Zhao, Y.; Wang, D.; Cai, Y. Toward Rapid Aqueous RAFT Polymerization of Primary Amine Functional Monomer under Visible Light Irradiation at 25°C. *Polym. Chem.* **2013**, *4* (4), 1176−1182.
(175) Fu, Q.; Ranji-Burachaloo, H.; Liu, M.; McKenzie, T. G.; Tan, S.; Reyhani, A.; Nothling, M. D.; Dunstan, D. E.; Qiao, G. G. Controlled RAFT Polymerization Facilitated by a Nanostructured Enzyme Mimic. *Polym. Chem.* **2018**, *9* (35), 4448−4454.
(176) Zhu, Y.; Egap, E. PET-RAft Polymerization Catalyzed by Cadmium Selenide Quantum Dots (Qds):: Grafting-from Qds

Photocatalysts to Make Polymer Nanocomposites. *Polym. Chem.* **2020**, *11* (5), 1018−1024.
(177) Liang, Y.; Ma, H.; Zhang, W.; Cui, Z.; Fu, P.; Liu, M.; Qiao, X.; Pang, X. Size Effect of Semiconductor Quantum Dots as Photocatalysts for PET-RAFT Polymerization. *Polym. Chem.* **2020**, *11* (31), 4961−4967.
(178) McClelland, K. P.; Clemons, T. D.; Stupp, S. I.; Weiss, E. A. Semiconductor Quantum Dots Are Efficient and Recyclable Photocatalysts for Aqueous PET-RAFT Polymerization. *ACS Macro Lett.* **2020**, *9* (1), 7−13.
(179) Lian, S.; Weinberg, D. J.; Harris, R. D.; Kodaimati, M. S.; Weiss, E. A. Subpicosecond Photoinduced Hole Transfer from a CdS Quantum Dot to a Molecular Acceptor Bound Through an Exciton-Delocalizing Ligand. *ACS Nano* **2016**, *10* (6), 6372−6382.
(180) Hu, L.; Wang, Q.; Zhang, X.; Zhao, H.; Cui, Z.; Fu, P.; Liu, M.; Liu, N.; He, S.; Pang, X.; Qiao, X. Light and Magnetism Dual-Gated Photoinduced Electron Transfer-Reversible Addition-Fragmentation Chain Transfer (PET-RAFT) Polymerization. *RSC Adv.* **2020**, *10* (12), 6850−6857.
(181) Wang, Q.; Hu, L.; Cui, Z.; Fu, P.; Liu, M.; Qiao, X.; Pang, X. Dual Roles of Amino Functionalized Silicon Quantum Dots (SiQDs) for Visible Light-Induced Surface Initiated PET-RAFT Polymerization on Substrates. *ACS Appl. Mater. Interfaces* **2020**, *12* (37), 42161−42168.
(182) Liang, E.; Liu, M.; He, B.; Wang, G.-X. ZnO as Photocatalyst for Photoinduced Electron Transfer-Reversible Addition-Fragmentation Chain Transfer of Methyl Methacrylate. *Adv. Polym. Technol.* **2018**, *37* (8), 2879−2884.
(183) Cheng, B. F.; Wang, L. H.; You, Y. Z. Photoinduced Electron Transfer-Reversible Addition-Fragmentation Chain Transfer (PET-RAFT) Polymerization Using Titanium Dioxide. *Macromol. Res.* **2016**, *24* (9), 811−815.
(184) McKenzie, T. G.; Fu, Q.; Wong, E. H. H.; Dunstan, D. E.; Qiao, G. G. Visible Light Mediated Controlled Radical Polymerization in the Absence of Exogenous Radical Sources or Catalysts. *Macromolecules* **2015**, *48* (12), 3864−3872.
(185) Fu, Q.; Xie, K.; McKenzie, T. G.; Qiao, G. G. Trithiocarbonates as Intrinsic Photoredox Catalysts and RAFT Agents for Oxygen Tolerant Controlled Radical Polymerization. *Polym. Chem.* **2017**, *8* (9), 1519−1526.
(186) Shanmugam, S.; Xu, J.; Boyer, C. Exploiting Metalloporphyrins for Selective Living Radical Polymerization Tunable over Visible Wavelengths. *J. Am. Chem. Soc.* **2015**, *137* (28), 9174−9185.
(187) Shanmugam, S.; Xu, J.; Boyer, C. Light-Regulated Polymerization under Near-Infrared/Far-Red Irradiation Catalyzed by Bacteriochlorophyll *A*. *Angew. Chem., Int. Ed.* **2016**, *55* (3), 1036−1040.
(188) Kettling, F.; Vonhören, B.; Krings, J. A.; Saito, S.; Ravoo, B. J. One-Step Synthesis of Patterned Polymer Brushes by Photocatalytic Microcontact Printing. *Chem. Commun.* **2015**, *51* (6), 1027−1030.
(189) Groenendaal, L.; Zotti, G.; Aubert, P. H.; Waybright, S. M.; Reynolds, J. R. Electrochemistry of Poly(3,4-Alkylenedioxythiophene) Derivatives. *Adv. Mater.* **2003**, *15* (11), 855−879.
(190) Guo, C. X.; Wang, M.; Chen, T.; Lou, X. W.; Li, C. M. A Hierarchically Nanostructured Composite of MnO2/Conjugated Polymer/Graphene for High-Performance Lithium Ion Batteries. *Adv. Energy Mater.* **2011**, *1* (5), 736−741.
(191) Kobayashi, N.; Teshima, K.; Hirohashi, R. Conducting Polymer Image Formation with Photoinduced Electron Transfer Reaction. *J. Mater. Chem.* **1998**, *8* (3), 497−506.
(192) Cai, X.; Anyaogu, K. C.; Neckers, D. C. Photopolymerization of Gold Nanoparticles: Size-Related Charge Separation and Emission. *J. Am. Chem. Soc.* **2007**, *129* (37), 11324−11325.
(193) Strandwitz, N. C.; Nonoguchi, Y.; Boettcher, S. W.; Stucky, G. D. In Situ Photopolymerization of Pyrrole in Mesoporous TiO2. *Langmuir* **2010**, *26* (8), 5319−5322.
(194) Goubard, F.; Aubert, P.-H.; Boukerma, K.; Pauthe, E.; Chevrot, C. Elaboration of Nanohybrid Materials by Photopolymerisation of 3,4-Ethylenedioxythiophene on TiO2. *Chem. Commun.* **2008**, *0* (27), 3139.
(195) Martins, C. R.; De Almeida, Y. M.; Do Nascimento, G. C.; De Azevedo, W. M. Metal Nanoparticles Incorporation during the Photopolymerization of Polypyrrole. *J. Mater. Sci.* **2006**, *41* (22), 7413−7418.
(196) Yang, X.; Lu, Y. Preparation of Polypyrrole-Coated Silver Nanoparticles by One-Step UV-Induced Polymerization. *Mater. Lett.* **2005**, *59* (19−20), 2484−2487.
(197) Bagheri, A.; Jin, J. Photopolymerization in 3D Printing. *ACS Appl. Polym. Mater.* **2019**, *1* (4), 593−611.
(198) Zhang, J.; Xiao, P. 3D Printing of Photopolymers. *Polym. Chem.* **2018**, *9* (13), 1530−1540.
(199) Layani, M.; Wang, X.; Magdassi, S. Novel Materials for 3D Printing by Photopolymerization. *Adv. Mater.* **2018**, *30* (41), 1706344.
(200) Pawar, A. A.; Saada, G.; Cooperstein, I.; Larush, L.; Jackman, J. A.; Tabaei, S. R.; Cho, N.-J.; Magdassi, S. High-Performance 3D Printing of Hydrogels by Water-Dispersible Photoinitiator Nanoparticles. *Sci. Adv.* **2016**, *2* (4), No. e1501381.
(201) Potapova, I.; Mruk, R.; Hübner, C.; Zentel, R.; Basché, T.; Mews, A. CdSe/ZnS Nanocrystals with Dye-Functionalized Polymer Ligands Containing Many Anchor Groups. *Angew. Chem., Int. Ed.* **2005**, *44* (16), 2437−2440.
(202) Ai, Q.; Fang, Q.; Liang, J.; Xu, X.; Zhai, T.; Gao, G.; Guo, H.; Han, G.; Ci, L.; Lou, J. Lithium-Conducting Covalent-Organic-Frameworks as Artificial Solid-Electrolyte-Interphase on Silicon Anode for High Performance Lithium Ion Batteries. *Nano Energy* **2020**, *72*, 104657.
(203) Zhu, D.; Xu, G.; Barnes, M.; Li, Y.; Tseng, C.-P.; Zhang, Z.; Zhang, J.-J.; Zhu, Y.; Khalil, S.; Rahman, M. M.; Verduzco, R.; Ajayan, P. M. Covalent Organic Frameworks for Batteries. *Adv. Funct. Mater.* **2021**, 2100505.
(204) Skaff, H.; Sill, K.; Emrick, T. Quantum Dots Tailored with Poly(Para-Phenylene Vinylene). *J. Am. Chem. Soc.* **2004**, *126* (36), 11322−11325.
(205) Zhu, D.; Zhu, Y.; Yan, Q.; Barnes, M.; Liu, F.; Yu, P.; Tseng, C.-P.; Tjahjono, N.; Huang, P.-C.; Rahman, M. M.; Egap, E.; Ajayan, P. M.; Verduzco, R. Pure Crystalline Covalent Organic Framework Aerogels. *Chem. Mater.* **2021**, *33* (11), 4216−4224.
(206) Kumar, S. K.; Benicewicz, B. C.; Vaia, R. A.; Winey, K. I. 50th Anniversary Perspective: Are Polymer Nanocomposites Practical for Applications? *Macromolecules* **2017**, *50* (3), 714−731.
(207) Green, M. Semiconductor Quantum Dots as Biological Imaging Agents. *Angew. Chem., Int. Ed.* **2004**, *43* (32), 4129−4131.
(208) Liu, M.; Ishida, Y.; Ebina, Y.; Sasaki, T.; Aida, T. Photolatently Modulable Hydrogels Using Unilamellar Titania Nanosheets as Photocatalytic Crosslinkers. *Nat. Commun.* **2013**, *4* (1), 2029.
(209) Liu, J.; An, T.; Chen, Z.; Wang, Z.; Zhou, H.; Fan, T.; Zhang, D.; Antonietti, M. Carbon Nitride Nanosheets as Visible Light Photocatalytic Initiators and Crosslinkers for Hydrogels with Thermoresponsive Turbidity. *J. Mater. Chem. A* **2017**, *5* (19), 8933−8938.
(210) Sun, J.; Schmidt, B. V. K. J.; Wang, X.; Shalom, M. Self-Standing Carbon Nitride-Based Hydrogels with High Photocatalytic Activity. *ACS Appl. Mater. Interfaces* **2017**, *9* (3), 2029−2034.
(211) Ye, B.; Yao, C.; Yan, M.; Zhang, H.; Xi, F.; Liu, J.; Li, B.; Dong, X. Photo-Induced Hydrogel Formation Based on g-C3N4 Nanosheets with Self-Cross-Linked 3D Framework for UV Protection Application. *Macromol. Mater. Eng.* **2019**, *304* (1), 1800500.
(212) Jiang, W.; Luo, W.; Zong, R.; Yao, W.; Li, Z.; Zhu, Y. Polyaniline/Carbon Nitride Nanosheets Composite Hydrogel: A Separation-Free and High-Efficient Photocatalyst with 3D Hierarchical Structure. *Small* **2016**, *12* (32), 4370−4378.
(213) Zhang, D.; Yang, J.; Bao, S.; Wu, Q.; Wang, Q. Semiconductor Nanoparticle-Based Hydrogels Prepared via Self-Initiated Polymerization under Sunlight, Even Visible Light. *Sci. Rep.* **2013**, *3* (1), 1399.
(214) Ulku, I.; Morlet-Savary, F.; Lalevée, J.; Yagci Acar, H. Homogenous Photopolymerization of Acrylic Monomers Initiated

with ZnO-Methacrylate in Non-Aqueous Medium and Production of Luminescent Nanocomposites. *Polym. Chem.* **2018**, *9* (7), 828−833.
(215) Buz, E.; Morlet-Savary, F.; Lalevée, J.; Acar, H. Y. CdS-Oleic Acid Quantum Dots as Long-Wavelength Photoinitiators in Organic Solvent and Preparation of Luminescent, Colloidal CdS/Polymer Nanocomposites. *Macromol. Chem. Phys.* **2018**, *219* (2), 1700356.
(216) Zhu, Y.; Zhu, D.; Yan, Q.; Gao, G.; Xu, J.; Liu, Y.; Alahakoon, S. B.; Rahman, M. M.; Ajayan, P. M.; Egap, E.; Verduzco, R. Metal Oxide Catalysts for the Synthesis of Covalent Organic Frameworks and One-Step Preparation of Covalent Organic Framework-Based Composites. *Chem. Mater.* **2021**, DOI: 10.1021/acs.chemmater.1c01747.
(217) Yan, J.; Pan, X.; Schmitt, M.; Wang, Z.; Bockstaller, M. R.; Matyjaszewski, K. Enhancing Initiation Efficiency in Metal-Free Surface-Initiated Atom Transfer Radical Polymerization (SI-ATRP). *ACS Macro Lett.* **2016**, *5* (6), 661−665.
(218) Wang, X.; Lu, Q.; Wang, X.; Joo, J.; Dahl, M.; Liu, B.; Gao, C.; Yin, Y. Photocatalytic Surface-Initiated Polymerization on TiO 2 toward Well-Defined Composite Nanostructures. *ACS Appl. Mater. Interfaces* **2016**, *8* (1), 538−546.
(219) Xie, Z.; Deng, X.; Liu, B.; Huang, S.; Ma, P.; Hou, Z.; Cheng, Z.; Lin, J.; Luan, S. Construction of Hierarchical Polymer Brushes on Upconversion Nanoparticles via NIR-Light-Initiated RAFT Polymerization. *ACS Appl. Mater. Interfaces* **2017**, *9* (36), 30414−30425.
(220) Xu, J.; Shanmugam, S.; Boyer, C. Organic Electron Donor-Acceptor Photoredox Catalysts: Enhanced Catalytic Efficiency toward Controlled Radical Polymerization. *ACS Macro Lett.* **2015**, *4* (9), 926−932.
(221) Deeb, C.; Ecoffet, C.; Bachelot, R.; Plain, J.; Bouhelier, A.; Soppera, O. Plasmon-Based Free-Radical Photopolymerization: Effect of Diffusion on Nanolithography Processes. *J. Am. Chem. Soc.* **2011**, *133* (27), 10535−10542.
(222) Minamimoto, H.; Toda, T.; Futashima, R.; Li, X.; Suzuki, K.; Yasuda, S.; Murakoshi, K. Visualization of Active Sites for Plasmon-Induced Electron Transfer Reactions Using Photoelectrochemical Polymerization of Pyrrole. *J. Phys. Chem. C* **2016**, *120* (29), 16051−16058.
(223) Guselnikova, O.; Marque, S. R. A.; Tretyakov, E. V.; Mares, D.; Jerabek, V.; Audran, G.; Joly, J.-P.; Trusova, M.; Svorcik, V.; Lyutakov, O.; Postnikov, P. Unprecedented Plasmon-Induced Nitroxide-Mediated Polymerization (PI-NMP): A Method for Preparation of Functional Surfaces. *J. Mater. Chem. A* **2019**, *7* (20), 12414−12419.
(224) Erzina, M.; Guselnikova, O.; Postnikov, P.; Elashnikov, R.; Kolska, Z.; Miliutina, E.; Švorčík, V.; Lyutakov, O. Plasmon-Polariton Induced, "from Surface" RAFT Polymerization, as a Way toward Creation of Grafted Polymer Films with Thickness Precisely Controlled by Self-Limiting Mechanism. *Adv. Mater. Interfaces* **2018**, *5* (22), 1801042.
(225) Zhang, J.; Huang, Y.; Wang, D.; Pollard, A. C.; Chen, Z. G.; Egap, E. Triblock Near-Infrared Fluorescent Polymer Semiconductor Nanoparticles for Targeted Imaging. *J. Mater. Chem. C* **2017**, *5* (23), 5685−5692.
(226) Pinkas, A.; Waiskopf, N.; Gigi, S.; Naor, T.; Layani, A.; Banin, U. Morphology Effect on Zinc Oxide Quantum Photoinitiators for Radical Polymerization. *Nanoscale* **2021**, *13* (15), 7152−7160.
(227) Zhao, F.; Li, N.; Zhu, Y.-F.; Han, Z.-Y. Enantioselective Construction of Functionalized Tetrahydrocarbazoles Enabled by Asymmetric Relay Catalysis of Gold Complex and Chiral Brønsted Acid. *Org. Lett.* **2016**, *18* (7), 1506−1509.
(228) Du, Y.-L.; Hu, Y.; Zhu, Y.-F.; Tu, X.-F.; Han, Z.-Y.; Gong, L.-Z. Chiral Gold Phosphate Catalyzed Tandem Hydroamination/Asymmetric Transfer Hydrogenation Enables Access to Chiral Tetrahydroquinolines. *J. Org. Chem.* **2015**, *80* (9), 4754−4759.
(229) Du, Y.-L.; Zhu, Y.-F.; Han, Z.-Y. Pd(II)-Catalyzed Cycloisomerization/Dipolar Cycloaddition Cascade of *N* -Arylnitrone Alkynes with Olefins. *J. Org. Chem.* **2015**, *80* (15), 7732−7738.
(230) Gan, W.; Xu, H.; Jin, X.; Cao, X.; Gao, H. Recyclable Palladium-Loaded Hyperbranched Polytriazoles as Efficient Polymer Catalysts for Heck Reaction. *ACS Appl. Polym. Mater.* **2020**, *2* (2), 677−684.
(231) Mori, K.; Taga, T.; Yamashita, H. Isolated Single-Atomic Ru Catalyst Bound on a Layered Double Hydroxide for Hydrogenation of CO2 to Formic Acid. *ACS Catal.* **2017**, *7* (5), 3147−3151.
(232) Gao, G.; Jiao, Y.; Waclawik, E. R.; Du, A. Single Atom (Pd/Pt) Supported on Graphitic Carbon Nitride as an Efficient Photocatalyst for Visible-Light Reduction of Carbon Dioxide. *J. Am. Chem. Soc.* **2016**, *138* (19), 6292−6297.
(233) Buss, B. L.; Lim, C. H.; Miyake, G. M. Dimethyl Dihydroacridines as Photocatalysts in Organocatalyzed Atom Transfer Radical Polymerization of Acrylate Monomers. *Angew. Chem., Int. Ed.* **2020**, *59* (8), 3209−3217.
(234) Wu, X.; Xie, S.; Liu, C.; Zhou, C.; Lin, J.; Kang, J.; Zhang, Q.; Wang, Z.; Wang, Y. Ligand-Controlled Photocatalysis of CdS Quantum Dots for Lignin Valorization under Visible Light. *ACS Catal.* **2019**, *9* (9), 8443−8451.
(235) Oliver, S.; Zhao, L.; Gormley, A. J.; Chapman, R.; Boyer, C. Living in the Fast Lane-High Throughput Controlled/Living Radical Polymerization. *Macromolecules* **2019**, *52* (1), 3−23.
(236) Lamb, J. R.; Qin, K. P.; Johnson, J. A. Visible-Light-Mediated, Additive-Free, and Open-to-Air Controlled Radical Polymerization of Acrylates and Acrylamides. *Polym. Chem.* **2019**, *10* (13), 1585−1590.
(237) McCarthy, B.; Miyake, G. M. Organocatalyzed Atom Transfer Radical Polymerization Catalyzed by Core Modified *N* -Aryl Phenoxazines Performed under Air. *ACS Macro Lett.* **2018**, *7* (8), 1016−1021.
(238) Pal, A.; Ghosh, I.; Sapra, S.; König, B. Quantum Dots in Visible-Light Photoredox Catalysis: Reductive Dehalogenations and C-H Arylation Reactions Using Aryl Bromides. *Chem. Mater.* **2017**, *29* (12), 5225−5231.
(239) Buss, B. L.; Miyake, G. M. Photoinduced Controlled Radical Polymerizations Performed in Flow: Methods, Products, and Opportunities. *Chem. Mater.* **2018**, *30* (12), 3931−3942.